2012

Rate-Based Robust Adaptive Performance Tracking Control Of Network Flows

Xiaoyan Mei
North Carolina Agricultural and Technical State University

RATE-BASED ROBUST ADAPTIVE PERFORMANCE TRACKING CONTROL OF NETWORK FLOWS

by

Xiaoyan Mei

A dissertation submitted to the graduate faculty
in partial fulfillment of the requirements for the degree of
DOCTOR OF PHILOSOPHY

Department: Electrical and Computer Engineering
Major: Electrical Engineering
Major Professor: Dr. Marwan U. Bikdash

North Carolina A&T State University
Greensboro, North Carolina
2012

ABSTRACT

Mei, Xiaoyan. RATE-BASED ROBUST ADAPTIVE PERFORMANCE TRACKING CONTROL OF NETWORK FLOWS. (**Major Professor: Dr. Marwan U. Bikdash**), North Carolina Agricultural and Technical State University.

Network flow control methods have been studied for years to ensure the efficient usage of network resources. By adopting a representation reminiscent of the sliding surface representation, this work explores a highly adaptive network flow control strategy. The rate-based network flow control scheme is investigated through a novel model description in the matrix notation, and guaranteed to be stable under mild assumptions. The control law has a simple form but the proof of robust stability is quite involved via the Lyapunov theory. Simulations demonstrated that the developed adaptive algorithms are robust and effective in maintaining good link price and backlog tracking precision, with both constant and time-varying reference source rate inputs. The robustness and adaptation of the designed control law were also investigated in the presence of uncertain state dynamics and external disturbances. The salient feature of the proposed approach is its simple design procedures, easy real-time implementation and less on-line computations.

The proposed algorithm was tested using simple network models as well as using more realistic models such as those developed using the small-world network topologies.

School of Graduate Studies

North Carolina Agricultural and Technical State University

This is to certify that the Doctoral Dissertation of

Xiaoyan Mei

has met the dissertation requirements of
North Carolina Agricultural and Technical State University

Greensboro, North Carolina
2012

Approved by:

Dr. Marwan U. Bikdash Major Professor	Dr. Gary L. Lebby Committee Member
Dr. Robert Y. Li Committee Member	Dr. Abdollah Homaifar Committee Member
Dr. Clinton B. Lee Committee Member	Dr. John C. Kelly Department Chairperson

Dr. Sanjiv Sarin
Associate Vice Chancellor for Research and Dean of Graduate Studies

DEDICATION

This work is dedicated to my husband Fujiang Huang, daughter Melissa Huang, my parents, Wanrui Mei and Guihua Yang, elder sister, Yan Mei, brother-in-law, Liangzhou Liao, and nephew Wenjun Liao, younger sister Dan Mei, parents-in-law, Guihua Huang and Xianqiong Jiang, my advisor of Master of Science degree Prof. Zhi Yang and his wife Lei Bi, and my great grandparents Prof. Jiajun Mei and Prof. Zhijing Zhou for their inspiration and unflinching support through my years of education.

BIOGRAPHICAL SKETCH

Xiaoyan Mei was born on October 27, 1979, in Anlu, Hubei Province, China. She received the Bachelor of Science degree in Measurement and Control Technology and Instrumentation from Wuhan Institute of Technology, Wuhan, China, in 2003. She received the Master of Science degree in Pattern Recognition and Intelligent System from Chongqing University, Chongqing, China, in 2006. She joined the Department of Electrical and Computer Engineering at the North Carolina Agricultural and Technical State University, Greensboro, North Carolina, in spring 2007 for the Doctor of Philosophy degree in Electrical Engineering. She has been working in the Advanced Robotics Laboratory under the supervision of Dr. Marwan. U. Bikdash since fall 2008.

ACKNOWLEDGMENTS

He who learns from a colleague a single chapter, a single law, a single verse, a single statement, or even a single letter, ought to pay him honor.

— Pirkei Avot

My deepest appreciation will present to Dr. Marwan U. Bikdash, my major advisor, who is so knowledgeable and has been extremely patient and instructive in advising me with my research. Support from Pennsylvania State University and The Defense Threat Reduction Agency (DTRA) by contract DTRA01-03-D-0010/0020 and sub-contract S03-34 is gratefully acknowledged.

My thanks also go to Dr. Gary L. Lebby, Dr. Abdollah Homaifar, Dr. Robert Y. Li, Dr. Clinton B. Lee, Dr. Jung H. Kim, and Dr. John Kelly for their outstanding advice and encouragement.

I am grateful to my friends May L. Vansteen, Robert Vansteen, Zonghong Han, Mingjin Zhang, Dr. Man Yang, Ruijun Zou, Lina bai, Ling Ren, Yang Liu, Beibei Liu, Jiaying Li, Dr. Lixin Fu, Dr. Shuangning Xiu, Dr. Xiaomei Liu, Dr. Zhaoqiong Qin, Qianping He, Dr. Yaohang Li, Dr. Liangjing Wu, Dr. Jia Li, Yuqiang Long, Zixu Zhang, and Shu Wan, who helped me so much during the past years in Greensboro.

I would also take this opportunity to acknowledge my thankfulness to peer students Wenchuan Cai, Teshome Feyessa, Meng Vang, Serap Karagol, Burak Cetin, Ran Zhang, Pravin Chopade, David Tettey, Wogayehu Yeshitila, Dado Karim Sylla, Wald Iloylan, and Joutel S Amrani Sliman for their assistance and companionship of my study.

TABLE OF CONTENTS

LIST OF FIGURES

FIGURE **PAGE**

LIST OF TABLES

TABLE **PAGE**

CHAPTER 1
INTRODUCTION

Today's society is growing increasingly dependent upon large-scale, highly distributed systems that operate in unbounded network environments. Unbounded networks, such as the transportation network, communication network, etc., is in urgent need an intelligent administrative control and unified security protocol to react when subjected to multiple failures [1]. Flow control is one of the most important dynamic processes adopted to avoid congestions in an unbounded network.

1.1 Literature Review

In general, flow control methods were classified into two types: preventive control and reactive control [2]. The aim of the preventive control is to protect the network from becoming overload by using static resource allocation, as opposed to an adaptive resource allocation. A reactive flow controller endeavours to prevent the congestion when it senses a tendency towards congestion by employing a closed-loop feedback control mechanism, thus ensuring efficient use of network resources.

Rate-based and credit-based flow controls are two classes of reactive network flow control schemes [3]. Rate-based flow control strategies manipulate the transmission rate by controlling the rate of traffic entering the network. There has been a large collection of mathematical techniques dedicated to the design and analysis of network rate-control and flow optimization aiming to maximize network utility. An important generalized rate-

control algorithm [4] provided a mathematical formulation for two concepts of communication flow control algorithms in terms of the primal and dual forms. Their work also addressed the stability, proportional equilibrium fairness, and routing control problems with respect to queue signals and shadow prices, as well as studies on the consequences of stochastic disturbance and time delays. Low and Lapsley [5] discussed an optimization algorithm to maximize the aggregate source utility over transmission rate subject to link capacity constraints. Convergence to globally optimal tracking was achieved when the network is slowly varying. To maximize aggregate utility, Low [6] proposed a distributed primal-dual algorithm that treated source rate as a primal variable. The algorithm responds to congestion in the path and uses congestion measures as a dual feedback to sources that use the link. Low [6] focused mainly on the analysis of the equilibrium properties of various Transmission Control Protocol (TCP) / Active Queue Management (AQM) protocols while ignoring the stability and dynamics discussion.

A cross-layer dual optimization algorithm which considers the equilibrium properties of TCP and an active queue management scheme were given in [7] and [8]. They show a trade-off between equilibrium stability of dynamic routing and utility maximization. A limited utility can be achieved by adding a static term to the link cost to ensure stability. Therefore, the layering of single-path routing can achieve the same utility. Multipath routing was introduced as a decomposition of the utility optimization over source rates and routes.

Various heuristics for stable and robust networks are proposed by Paganini [9] and [10]. Athuraliya [11] considered the problem of random exponential marking to decou-

ple congestion measures from performance measures aiming to get high utilization with less loss and delays. Wen and Arcak [12] presented a unifying passivity formulation of the problem of stabilizing source and link control, with a combination of primal/dual congestion control, as to ensure robustness in stability and performance with respect to time delays, uncertain flows and varying capacity.

Another network flow control method based on the pricing signal strategy was presented by Paganini [13], in which linearization around the source rate equilibrium was attempted to discuss stability and capacity-variation tracking. Recently some intelligent route-guidance and trajectory planning methodologies have been designed to address the Dynamic Traffic Assignment and Dynamic Traffic Routing problems [14] - [21].

However, adaptive algorithms have not been developed for source control or routing control. A source control algorithm will be derived in this dissertation and they will be able to neutralize the effect of uncertainties and disturbances from unknown local traffic or from outside of the controlled network, while at the same time guarantee robust asymptotic stability.

1.2 Research Motivation

Indirect adaptive controllers have been shown to provide stability and asymptotic tracking of a reference signal for a wide class of continuous-time nonlinear plants with zero or non-zero dynamics, uncertainties and unmodeled fault or disturbances, provided that the state error in representing the nonlinear plant dynamics converges to zero or compact regions [22] - [27]. Encouraged by the tracking control spirit of Song [23], the focus

of this work will be on new network flow control algorithms that exhibit intelligent attributes such as robustness, adaptation, tracking, and have reasonable performance under extreme complex and changing operating environments. Inspirations drawn from communication network control will be used to develop these novel control schemes. A filtered error vector reminiscent of the sliding mode control methodology is employed in this work not only to ensure control precision and good dynamic tracking performance, but also to take care of (i) the high degree of uncertainties in the network itself and in the environment; (ii) the large operation envelope of the network, and (iii) the high performance demands in terms of reliability and adaptation.

The primary objective of this work is to find a source-rate control vector that can mitigate the effect of unknown traffic generated from outside of the controlled sources and the effect of unknown local traffic. However, this control must possess asymptotic stability. The framework we adopt in this work is more complex than that studied in the research alluded to above. Here, a network consisting of an arbitrary number of bottleneck resources is investigated. Global asymptotic stability was demonstrated theoretically using Lyapunov stability and through simulations.

This dissertation is organized as follows:

1 A review of a basic continuous-time network model with a specific example is given in Chapter 2.

2 The set of possible equilibrium conditions of the studied model was reduced in Chapter 3.

3 Based on a novel matrix notation of the nonlinear model, Chapter 4 develops an

adaptive control scheme to ensure robust network flow tracking performance to meet the expected network equilibria. The adaptation and stability of the proposed control law are proved by adopting Lyapunov theory and the robustness and reliability are investigated by simulations in Matlab.

4 Further investigations of the designed control scheme in terms of counteracting the harsh effect of uncertainties and disturbances are studied in Chapter 5.

5 A small-world network concept is introduced in Chapter 6 to verify the robustness and adaptation in a more practical stressed network topology.

6 Chapter 7 concludes this dissertation with a summary of the key results, conclusions and future work possibilities.

CHAPTER 2
MODEL OF THE NETWORK FLOW CONTROL

This chapter introduces a mathematical model representing the network dynamics and gives an example of the used model.

2.1 Network Model

A network is modeled as a set L of directed links with finite capacities $c = (c_l, l \in L)$, shared by a set K of origin-path-destination combinations, indexed by k; in this work we simply refer to an origin-path-destination combination as "source". There is a set $L_k \subseteq L$ of links used by source $k,$ and defined by a $L \times K$ routing matrix R_{lk}, with binary elements.

$$R_{lk} = \begin{cases} 1 & \text{if source } k \text{ uses link } l \\ 0 & \text{otherwise} \end{cases} .$$

For each link $l,$ we consider the following variables: the capacity c_l; the rate y_l of the aggregate flow through link l; the backlog or queue length b_l; and the price signal p_l.

For each route $k,$ we only discuss the route rate x_k and the aggregate price q_k of all links used by source k.

The framework of the network flow control model as shown in Figure 2.1 adopted in [4], [5], [12] and [13] is that the links only feed back the price information to the routes or sources that go through them:

$$y = Rx \iff y_l = \sum_l R_{lk} x_k, \tag{2.1}$$

$$q = R^T p \iff q_k = \sum_k R^T_{lk} p_l, \tag{2.2}$$

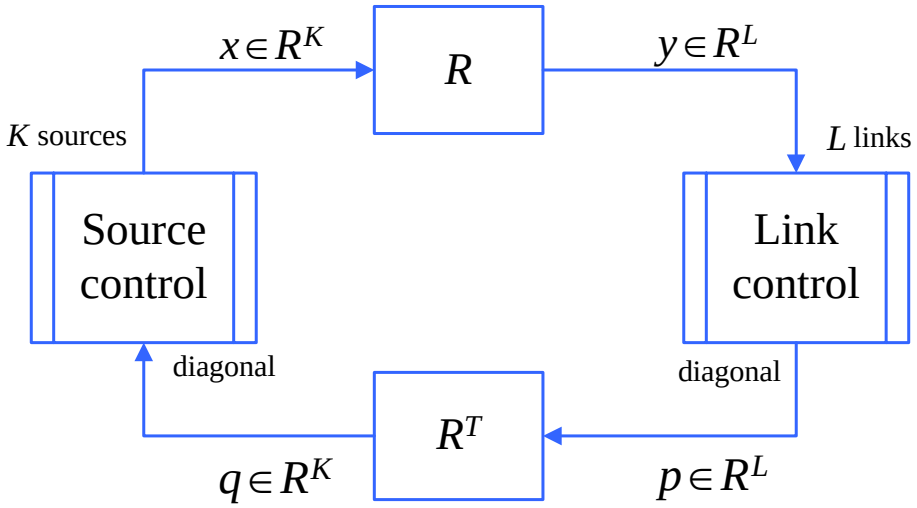

Figure 2.1. Model of network flow control

where $x_k \in \mathcal{R}^K$ is the flow generation rate corresponding to source k, $y_l \in \mathcal{R}^L$ is the aggregate rate of each link l, $p_l \in \mathcal{R}^L$ is the link price, and $q_k \in \mathcal{R}^K$ is the aggregate price of all the links used by a certain source k; $(\cdot^T)$ indicates transpose.

A typical strategy for flow control is to decompose the problem into a static utility optimization problem and a dynamic stabilization problem [4], [5]. For static source control, the optimization problem in [12] and [13] is to maximize the sum of the utility function $U_k(x_k)$ for the sources with respect to the capacity constraints in the links:

$$\max_{x \geq 0} \sum_{k=1}^{K} U_k(x_k) \text{ subject to } y = Rx \leq c. \tag{2.3}$$

The utility functions are assumed to be strictly concave and differentiable, which means that as the maximum is achieved at $x_k = U_k'^{-1}(q_k)$, where $U_k'^{-1}$ is the inverse func-

tion of the derivative of U_k, x_k is a strictly monotone decreasing function of q_k, because $U_k^{'}$ is strictly decreasing in $x_k > 0$.

The dynamic link price control is designed as a continuous-time version of price dynamics [13], for each link l:

$$\frac{db_l}{dt} = \begin{cases} (y_l - c_l) & \text{if } b_l(t) > 0 \\ [y_l - c_l]^+ & \text{if } b_l(t) = 0 \end{cases}, \tag{2.4}$$

$$\frac{dp_l}{dt} = \begin{cases} \gamma(\alpha_l b_l + y_l - c_l) & \text{if } p_l(t) > 0 \\ \gamma[\alpha_l b_l + y_l - c_l]^+ & \text{if } p_l(t) = 0 \end{cases}, \tag{2.5}$$

where$[z]^+ = \max\{0, z\}$, $\gamma > 0$ and $\alpha_l > 0$ are small constants.

According to [13], the source rate equation $x = f(q_k)$, where f_k is a strictly monotone decreasing function of q_k (2.2). When the aggregate price q_k of all the links used by a certain source k increases; consequently, the source rate x decreases, which means that the more severe the congestion, the smaller the aggregate rate.

The stability of flow control via source aggregate rate (2.3), link queue length rate (2.4) and link price rate (2.5), was theoretically analyzed [9], [10] and [13]. However, a simple method that can cope with the effect of uncertainty and disturbance from unknown local traffic or from outside of the controlled network, while at the same time maintain robust asymptotic stability, has not been studied yet. This work will introduce a new network flow control algorithm that can demonstrate intelligent attributes such as robustness, adaptation, stability, and are capable of counteracting the uncertain term, which is assumed to be bounded. The notations introduced throughout this work are summarized in Table 2.1.

Table 2.1. Notation

Notation	Definition
L, l	number of network links, link index
K, k	number of sources, source index
R, r	$L \times K$ dimension routing matrix, row vector index
b, b_l	traffic network backlog vector, link backlog index
p, p_l	traffic network price vector, link price index
y, y_l	aggregate rate vector, aggregate rate index
c, c_l	link capacity vector, link capacity index
e_1	error between backlog b and desired state b^d
e_2	error between price p and desired state p^d
s	designed sliding surface, $s = e_1 + \eta e_2$
$W \in \mathcal{R}^L$	a column vector representing traffic fluctuation and disturbance
H_1, h_{1l}	diagonal matrixes of $R^{L\times L}$ with h_{1l},sign function of b_l
H_2, h_{2l}	diagonal matrixes of $R^{L\times L}$ with h_{2l},sign function of p_l
H	$H = H_1 + \eta\gamma H_2$
Γ	represents the nonlinearity, disturbance and uncertainty of the system
μ	a known scalar shape function only depending on s
a	unknown but finite nonnegative constants need to be defined
Q	positive semidefinite matrix, $Q = HRR^T H^T$
V_1, V_2	Lyapunov candidate function
ε, η, ρ_0, σ, κ	control parameters introduced in the control law
k_1	average degree of connections for any arbitrary node
ρ	the probability of the edge be randomly rewired over the entire graph

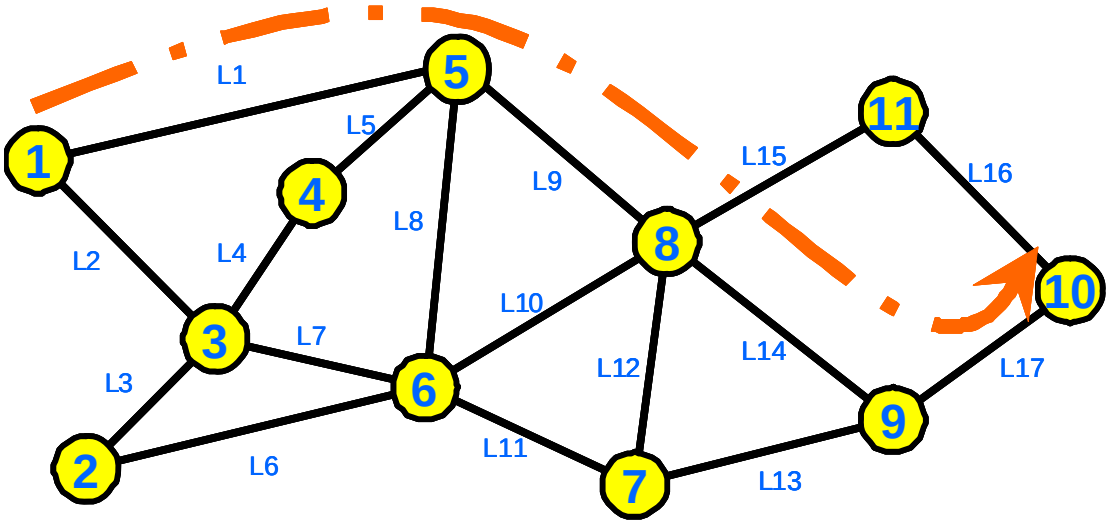

Figure 2.2. Traffic network with 17 links and 11 nodes

2.2 Network Example

This section will give out an example to illustrate the network model addressed as (2.1). The traffic network example illustrated in Figure 2.2 consists 11 nodes and 17 links, from which we randomly chose 10 sources of origin-path-destination and we assume that each route is in one direction. The detailed routes set of origin-path-destination demonstrated by both nodes and links are enumerated in the Table 2.2.

Table 2.2. Routes randomly choosen by origin-destination pairs

Origin Destination Pair	Source Number	Route 1 by Nodes	Route 1 by Links	Source Number	Route 2 by Nodes	Route 2 by Links
N_1 - N_{10}	k=1	1-5-8-11-10	1-9-15-16	k=2	1-3-6-7-9-10	2-7-11-13-17
N_1 - N_5	k=3	1-5	1	k=4	1-3-4-5	2-4-5
N_2 - N_{11}	k=5	2-3-4-5-8-11	3-4-5-9-15	k=6	2-6-8-11	6-10-15
N_5 - N_{10}	k=7	5-8-11-10	9-15-16	k=8	5-6-7-9-10	8-11-13-17
N_7 - N_{10}	k=9	7-8-11-10	12-15-16	k=10	7-9-10	13-17

The corresponding routing matrix of this traffic network is

$$R_{L\times K} = \begin{bmatrix} 1 & 0 & 1 & 0 & 0 & 0 & 0 & 0 & 0 & 0 \\ 0 & 1 & 0 & 1 & 0 & 0 & 0 & 0 & 0 & 0 \\ 0 & 0 & 0 & 0 & 1 & 0 & 0 & 0 & 0 & 0 \\ 0 & 0 & 0 & 1 & 1 & 0 & 0 & 0 & 0 & 0 \\ 0 & 0 & 0 & 1 & 1 & 0 & 0 & 0 & 0 & 0 \\ 0 & 0 & 0 & 0 & 0 & 1 & 0 & 0 & 0 & 0 \\ 0 & 1 & 0 & 0 & 0 & 0 & 0 & 0 & 0 & 0 \\ 0 & 0 & 0 & 0 & 0 & 0 & 0 & 1 & 0 & 0 \\ 1 & 0 & 0 & 0 & 1 & 0 & 1 & 0 & 0 & 0 \\ 0 & 0 & 0 & 0 & 0 & 1 & 0 & 0 & 0 & 0 \\ 0 & 1 & 0 & 0 & 0 & 0 & 0 & 1 & 0 & 0 \\ 0 & 0 & 0 & 0 & 0 & 0 & 0 & 0 & 1 & 0 \\ 0 & 1 & 0 & 0 & 0 & 0 & 0 & 1 & 0 & 1 \\ 0 & 0 & 0 & 0 & 0 & 0 & 0 & 0 & 0 & 0 \\ 1 & 0 & 0 & 0 & 1 & 1 & 1 & 0 & 1 & 0 \\ 1 & 0 & 0 & 0 & 0 & 0 & 1 & 0 & 1 & 0 \\ 0 & 1 & 0 & 0 & 0 & 0 & 0 & 1 & 0 & 1 \end{bmatrix}. \tag{2.6}$$

CHAPTER 3
THE EQUILIBRIUM POINTS

An important concept in dealing with the state equation is the concept of an equilibrium point. A point x^* in the state space is said to be an equilibrium point if it has the property that whenever the state of the system starts at x^* it will remain at x^* for all future time [22]. For the continuous-time dynamics in (2.4) and (2.5), the equilibrium points are the real roots of the equations

$$db_l/dt|_{b_l=b_l^*} = 0 \text{ or simply } \dot{b}_l = 0, \tag{3.1}$$

$$dp_l/dt|_{p_l=p_l^*} = 0 \text{ or simply } \dot{p}_l = 0. \tag{3.2}$$

We assume that at the equilibrium status, for each $l \in L$, $k \in K$, the expected aggregate rate of each link is y_l^* and of each source is x_k^*, respectively, and the expected backlogs and link price are b_l^*, p_l^*.

From (2.4), $\dot{b}_l = 0$ implies that

$$y_l = c_l \qquad \text{if } b_l > 0, \tag{3.3}$$

$$y_l \leq c_l \qquad \text{if } b_l = 0. \tag{3.4}$$

From (2.5), $\dot{p}_l = 0$ implies that

$$\alpha_l b_l + y_l - c_l = 0 \qquad \text{if } p_l > 0, \tag{3.5}$$

$$\alpha_l b_l + y_l - c_l \leq 0 \qquad \text{if } p_l = 0, \tag{3.6}$$

where $\alpha_l > 0$.

There are only two allowable equilibria conditions:

$$b_l = 0,\ p_l = 0,\ y_l \leq c_l, \tag{3.7}$$

$$b_l = 0,\ p_l > 0,\ y_l = c_l. \tag{3.8}$$

Note that the equilibrium

$$b_l > 0,\ p_l > 0 \tag{3.9}$$

is not allowed, because (3.3) implies that $y_l = c_l$, and hence (3.5) becomes $\alpha_l b_l = 0$, which contradicts $b_l > 0$.

Similarly, the equilibrium

$$b_l > 0,\ p_l = 0 \tag{3.10}$$

is also not allowed, because (3.3) implies that $y_l = c_l$, and hence (3.6) becomes $\alpha_l b_l \leq 0$, which contradicts $b_l > 0$.

Note that at the two allowable equilibria (3.7) and (3.8), the backlogs are zero but the link prices can be positive if the corresponding link flows equal to their capacities.

CHAPTER 4
ROBUST ADAPTIVE NETWORK PERFORMANCE TRACKING CONTROL

This chapter is dedicated to designing an adaptive robust-stable network performance tracking control strategy in the presence of uncertainties and disturbances from unknown local traffic or from outside of the controlled network. The uncertainties and disturbances are assumed to be bounded. The basic structure for implementing the adaptive control law is illustrated in Figure 4.1. A novel matrix denotation of the network model will be developed to simplify the design of adaptive controller.

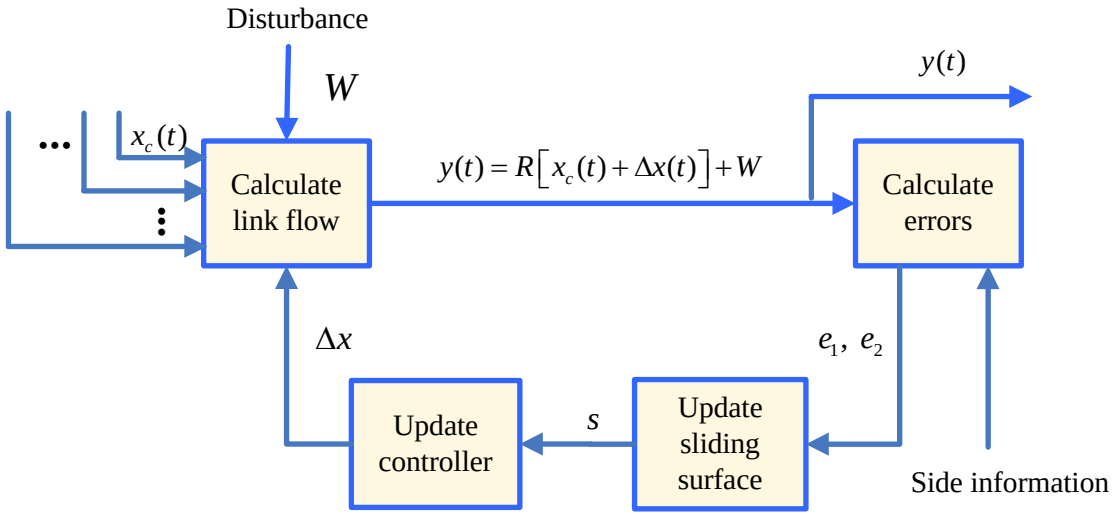

Figure 4.1. Basic structure of adaptive tracking control

4.1 Model in Matrix Notation

Before proposing the robust adaptive network performance tracking control algorithm, we discuss the continuous-time network model of (2.4) and (2.5). For reading convenience,

we repeat the model here. For each link l:

$$\frac{db_l}{dt} = \begin{cases} (y_l - c_l) & \text{if } b_l(t) > 0 \\ [y_l - c_l]^+ & \text{if } b_l(t) = 0 \end{cases}, \tag{4.1}$$

$$\frac{dp_l}{dt} = \begin{cases} \gamma(\alpha_l b_l + y_l - c_l) & \text{if } p_l(t) > 0 \\ \gamma[\alpha_l b_l + y_l - c_l]^+ & \text{if } p_l(t) = 0 \end{cases}, \tag{4.2}$$

where$[z]^+ = \max\{0, z\}$, $\gamma > 0$ and $\alpha_l > 0$ are small constants.

To facilitate the control design, we adopt the notation of switch function

$$\text{for } x \in \mathbb{R},\ \text{sgn}(x) = \begin{cases} \frac{x}{|x|} & x \neq 0 \\ 0 & x = 0 \end{cases},$$

and rewrite the dynamics of backlog (4.1) and link price (4.2) as:

$$\dot{b}_l = (y_l - c_l) \qquad \text{if } b_l(t) > 0, \tag{4.3}$$

$$\dot{b}_l = \frac{1}{2}(y_l - c_l)(1 + \text{sgn}(y_l - c_l)) \qquad \text{if } b_l(t) = 0, \tag{4.4}$$

$$\dot{p}_l = \gamma(\alpha_l b_l + y_l - c_l) \qquad \text{if } p_l(t) > 0, \tag{4.5}$$

$$\dot{p}_l = \frac{1}{2}\gamma[\alpha_l b_l + y_l - c_l](1 + \text{sgn}(\alpha_l b_l + y_l - c_l)) \qquad \text{if } p_l(t) = 0. \tag{4.6}$$

Let

$$\beta_{1l} = \frac{1}{2}(1 + \text{sgn}(y_l - c_l)), \tag{4.7}$$

$$\beta_{2l} = \frac{1}{2}(1 + \text{sgn}(\alpha_l b_l + y_l - c_l)), \tag{4.8}$$

where β_{1l} depends on the mismatch between the aggregate flow y_l and the link capacity c_l; β_{2l} depends on the difference between the sum of queue length b_l and the traffic flow of each link y_l and link capacity c_l. Please note that $\beta_{1l} = \frac{1}{2}$, $\beta_{2l} = \frac{1}{2}$ will make no influence

to the variations rate of queue length and link price at the moment $y_l = c_l$ and $\alpha_l b_l + y_l = c_l$.

$$\beta_{1l} = \begin{cases} 0 & \text{if } y_l < c_l \\ \frac{1}{2} & \text{if } y_l = c_l \\ 1 & \text{if } y_l > c_l \end{cases}, \tag{4.9}$$

$$\beta_{2l} = \begin{cases} 0 & \text{if } \alpha_l b_l + y_l < c_l \\ \frac{1}{2} & \text{if } \alpha_l b_l + y_l = c_l \\ 1 & \text{if } \alpha_l b_l + y_l > c_l \end{cases}. \tag{4.10}$$

In addition, the derivatives of the backlogs (4.3), (4.4), and the derivatives of link prices (4.5), (4.6), respectively, can be combined into

$$\dot{b}_l = (y_l - c_l)\left[\text{sgn}(b_l) + \beta_{1l}(1 - \text{sgn}(b_l))\right] \quad \text{if } b_l \geq 0, \tag{4.11}$$

$$\dot{p}_l = \gamma(\alpha_l b_l + y_l - c_l)\left[\text{sgn}(p_l) + \beta_{2l}(1 - \text{sgn}(p_l))\right] \quad \text{if } p_l \geq 0. \tag{4.12}$$

Furthermore, let

$$h_{1l} = \text{sgn}(b_l) + \beta_{1l}(1 - \text{sgn}(b_l)), \tag{4.13}$$

$$h_{2l} = \text{sgn}(p_l) + \beta_{2l}(1 - \text{sgn}(p_l)), \tag{4.14}$$

where h_{1l} depends on the sign of b_l and h_{2l} depends on the sign of p_l. They also depend on β_{1l} and β_{2l}, respectively. Moreover,

$$h_{1l} = \begin{cases} 1 & \text{if } b_l > 0 \\ \beta_{1l} & \text{if } b_l = 0 \end{cases}, \tag{4.15}$$

$$h_{2l} = \begin{cases} 1 & \text{if } p_l > 0 \\ \beta_{2l} & \text{if } p_l = 0 \end{cases}, \tag{4.16}$$

and therefore $h_{1l}, h_{2l} \in \left\{0, \frac{1}{2}, 1\right\}$. The rewritten dynamics of the backlogs (4.11) and link prices (4.12) are

$$\dot{b}_l = h_{1l}(y_l - c_l), \tag{4.17}$$

$$\dot{p}_l = \gamma h_{2l}(\alpha_l b_l + y_l - c_l). \tag{4.18}$$

Therefore, extending to the entire networks by using matrix notation, the dynamics of backlogs and link prices become

$$\dot{b} = H_1(y - c), \tag{4.19}$$

$$\dot{p} = \gamma H_2(\alpha b + y - c), \tag{4.20}$$

where

$$H_1 = diag(h_{11},\ h_{12},\ \cdots,\ h_{1l}), \tag{4.21}$$

$$H_2 = diag(h_{21},\ h_{22},\ \cdots,\ h_{2l}), \tag{4.22}$$

H_1, H_2 are $\mathcal{R}^{L\times L}$ diagonal matrices of h_{1l} as in (4.15), h_{2l} as in (4.16); α is the parameter vector of α_l ; and $b,\ p,\ y,\ c$ denote the vectors of the backlogs, costs, traffic flows and capacities of the traffic network.

4.2 Boundedness Analysis of Uncertainties and Disturbances

As previously noted in Section 1.1, it is difficult to know the dynamic traffic flow characteristics precisely. The flow tracking control problem is stated as: Design the source aggregate rate x based on $b,\ \dot{b},\ p,$ and $\dot{p}$ such that the actual traffic flow asymptotically

tracks the desired backlog b^d and the desired link price p^d in the existence of unknown or unmodeled flow and the block-form routing matrix.

To investigate the control design and stability analysis, we define the desired flow tracking in terms of backlogs and link prices as

$$Z^d = \begin{bmatrix} b^d \\ p^d \end{bmatrix},$$

and the tracking errors as

$$e = Z - Z^d = \begin{bmatrix} b - b^d \\ p - p^d \end{bmatrix} \triangleq \begin{bmatrix} e_1 \\ e_2 \end{bmatrix}. \tag{4.23}$$

A sliding mode, or sliding surface, is a switching (discontinuous) control method commonly employed in the variable structure control, in which switching functions need to be designed to keep the trajectory on the sliding surface for the sake of yielding the desired dynamics and consequently to enable the closed loop system to become insensitive to parameter variations and disturbances in the state space.

For the network flow control problem under consideration, we introduce a vector reminiscent of the sliding surface notation as

$$s = e_1 + \eta e_2 \quad \eta > 0, \tag{4.24}$$

where η is a positive small constant, errors e_1 and e_2 are defined in (4.23), $s \in \mathcal{R}^L$, and e_1, e_2 converge to a small compact set

$$S(e_1, e_2) = \{(e_1, e_2) \mid \ \|e_1\| \leq s_1, \ \ \|e_2\| \leq s_2\},$$

as time increases, $s_1 \geq 0$, $s_2 \geq 0$ are constants indicating tracking precision, here $\|\cdot\|$ denotes the Euclidean norm.

Due to the uncertainty and inevitability of traffic fluctuation, the traffic fluctuation is explicitly introduced into the aggregate rate [28]. We assume that the measured backbone traffic flow is x_c. The control strategy is to design a controller Δx to counteract the effect of uncertainties and disturbances, then function (2.1) turns out to be

$$\begin{aligned} y &= Rx + W \\ &= R(x_c + \Delta x) + W, \end{aligned} \tag{4.25}$$

where $y \in \mathcal{R}^L, x_c \in \mathcal{R}^K$ is a deterministic column vector representing backbone source rate, $\Delta x \in \mathcal{R}^K$ represents a column vector we need to design, $W \in \mathcal{R}^L$ is a column vector representing uncertainties and disturbances from unknown local traffic sources and from outside of the controlled network.

Using Matrix notation, the derivatives of tracking errors turn to be

$$\dot{e}_1 = \dot{b} - \dot{b}^d = H_1(y - c), \tag{4.26}$$

$$\dot{e}_2 = \dot{p} - \dot{p}^d = \gamma H_2(\alpha b + y - c) - \dot{p}^d, \tag{4.27}$$

where H_1 as in (4.21), H_2 as in (4.22) are $\mathcal{R}^{L\times L}$ diagonal matrices defined in Section 4.1.

For a feasible network traffic flow control, the desired backlog b^d and its rate of variation $\dot{b}^d$ should be zero, the link price p^d and its rate of variation $\dot{p}^d$ should be bounded. Therefore, we assume that

$$\left\|b^d\right\| = \left\|\dot{b}^d\right\| = 0, \ \left\|p^d\right\| \leq B_{p^d}, \text{ and } \left\|\dot{p}^d\right\| \leq B_{\dot{p}^d},$$

where B_{p^d} and $B_{\dot{p}^d}$ are non-negative constants, i.e. $B_{p^d} \geq 0$, $B_{\dot{p}^d} \geq 0$.

The derivative of sliding surface becomes

$$\begin{aligned} \dot{s} &= \dot{e}_1 + \eta \dot{e}_2 \\ &= H_1(y-c) + \eta\gamma H_2(\alpha b + y - c) - \eta\dot{p}^d \\ &= (H_1 + \eta\gamma H_2)R\Delta x + (H_1 + \eta\gamma H_2)(x_c + W - C) + \eta\gamma\alpha H_2 b - \eta\dot{p}^d \\ &= HR\Delta x + \Gamma(\cdot), \end{aligned} \tag{4.28}$$

where

$$\begin{aligned} H &= H_1 + \eta\gamma H_2 \\ &= diag(h_{11} + \eta\gamma h_{21}, h_{12} + \eta\gamma h_{22}, \cdots, h_{1l} + \eta\gamma h_{2l}), \end{aligned} \tag{4.29}$$

and

$$\Gamma(\cdot) = H(x_c + W - C) + \eta\gamma\alpha H_2 b - \eta\dot{p}^d, \tag{4.30}$$

where H is a diagonal matrix since H_1, H_2 are diagonal matrixes of $\mathcal{R}^{L\times L}$, and $H = H^T$. The lumped quantity $\Gamma(\cdot)$ represents the measured traffic flow as well as the nonlinearity, disturbances and uncertainties of the system, which are the main challenge of controller design and implementation.

Since $h_{1l},\ h_{2l} \in \left\{0, \frac{1}{2}, 1\right\}$, every diagonal factor of H has the form of $\left\{0, \frac{1}{2}, 1\right\} + \eta\gamma \left\{0, \frac{1}{2}, 1\right\}$. Hence, the induced Euclidean norm of H is

$$\begin{aligned} ||H|| &= \max\{h_{11} + \eta\gamma h_{21}, h_{12} + \eta\gamma h_{22}, \cdots, h_{1l} + \eta\gamma h_{2l}\} \\ &\leq 1 + \eta\gamma \end{aligned} \tag{4.31}$$

We assume the difference between external disturbances and capacities is bounded as

$$\|W - C\| \leq B_w, \tag{4.32}$$

where $B_w > 0$. The measured backbone traffic flow is bounded as

$$||x_c|| \leq B_x, \tag{4.33}$$

where $B_x > 0$. The Euclidean norm of the first term of $\Gamma(\cdot)$ (4.30) can be bounded as

$$\begin{aligned} \|H(x_c + W - C)\| &\leq (1 + \eta\gamma) \|x_c + W - C\| \\ &\leq (1 + \eta\gamma)(B_x + B_w), \end{aligned} \tag{4.34}$$

and the Euclidean norm of the second term of $\Gamma(\cdot)$ can be bounded as

$$\begin{aligned} \|\eta\gamma\alpha H_2 b\| &= \|\eta\gamma\alpha H_2 e_1\| \\ &\leq \eta\gamma\alpha \|H_2\| \|e_1\| \\ &\leq \eta\gamma\alpha \|H_2\| \|s\|, \end{aligned} \tag{4.35}$$

where $\|H_2\| \leq 1$ with respect to $h_{2l} \in \left\{0, \frac{1}{2}, 1\right\}$, $\|b\| = \|e_1\| \leq \|s\|$ with the assumption that $\left\|b^d\right\| = \left\|\dot{b}^d\right\| = 0$; Moreover, the Euclidean norm of the third term of $\Gamma(\cdot)$ is

$$\left\|\eta\dot{p}^d\right\| \leq \eta B_{\dot{p}^d}. \tag{4.36}$$

Therefore, combining (4.30), (4.34), (4.35) and (4.36) yields

$$\begin{aligned} \|\Gamma(\cdot)\| &\leq (1+\eta\gamma)(B_x + B_w) + \eta\gamma\alpha \|s\| + \eta B_{\dot{p}^d} \\ &= a_1 + a_2 \|s\| \\ &\leq a\mu, \end{aligned} \tag{4.37}$$

where a, a_1, a_2 are unknown but finite nonnegative constants and defined as

$$a_1 = (1+\eta\gamma)(x^d + w^d) + \eta\xi^d, \tag{4.38}$$

$$a_2 = \eta\gamma\alpha, \tag{4.39}$$

$$a = \max\{a_1, a_2\}, \tag{4.40}$$

and μ is a known scalar shape function only depending on s

$$\mu = 1 + \|s\|. \tag{4.41}$$

4.3 Robust Adaptive Network Performance Tracking Control

Note that, given the matrix

$$Q = HRR^T H^T, \tag{4.42}$$

where H is defined in (4.29). From standard linear algebra [25], if

$$s^T Q s = \alpha_0 ||s||^2, \tag{4.43}$$

then the positive scalar α_0 satisfies

$$0 < \sigma_{\min}(Q) \leq \alpha_0 \leq ||Q|| = \sigma_{\max}(Q), \tag{4.44}$$

where $\sigma_{\max}(Q) = ||Q||$ is the maximum singular value of Q. However, since Q and H can be singular, which implies that Q can be positive semidefinite, then $\sigma_{\min}(Q)$ the minimum singular value of Q can be zero.

We can now establish the main theorem of this work.

Theorem 4.1: For a network subjected to bounded uncertainties and disturbances assumptions as (4.32) - (4.41), the control strategy defined about a desired equilibrium

$$\Delta x = -\frac{\rho_0 + \rho_t}{\alpha_0} R^T H^T s, \tag{4.45}$$

with

$$\rho_t = \frac{\hat{a}\mu^2}{\|s\|\,\mu + \varepsilon}, \tag{4.46}$$

$$\dot{\hat{a}} = -\kappa\hat{a} + \sigma\frac{||s||^2\,\mu^2}{||s||\,\mu + \varepsilon}, \tag{4.47}$$

where $\rho_0 > 0$, $\mu > 0$, $\epsilon > 0$, $\kappa > 0$, and $\sigma > 0$ are constants parameters, α_0 is a positive scalar defined in (4.43), μ is given in (4.41), leads to the following stability results: (a) s, $\dot{s}$, and $(a - \hat{a})$ converge to a set containing origin, with the converge rate $e^{-\varsigma t}$ $(\varsigma > 0)$. (b) Besides, the tracking error of backlog and link price are bounded to the set

$$S = \{e_1, e_2\,|\|e_1\| \leq s_1,\ \ \|e_2\| \leq s_2\}$$

where $s_1 = \sqrt{\frac{d_1}{\varsigma}}$, $s_2 = \sqrt{\frac{d_1}{\eta^2\varsigma}}$, $d_1 = \frac{\kappa a^2}{2\sigma} + a\varepsilon$.

In this control law, s is a vector reminiscent of the sliding surface notation as defined in (4.24), $\sigma > 0$ in (4.47) is an adaptive gain chosen to adjust tracking precision, $\kappa > 0$ is

a parameter designed to ensure the boundedness of $\hat{a}$, and the term $-\kappa\hat{a}$ is introduced to make appropriate corrections to prevent parameter drift [23].

4.4 Proof of the Theorem

First, we introduce the following two Definitions and Lemma.

Definition 4.2: [26] A continuous function φ: $[0, r] \longmapsto \mathcal{R}^+$ (or φ: $[0, \infty) \longmapsto \mathcal{R}^+$) is said to belong to Class $\mathcal{K}$, $i.e.$, $\varphi \in \mathcal{K}$ if (i) $\varphi(0) = 0$ (ii) φ is strictly increasing on $[0, r]$ (or on $[0, \infty)$).

Definition 4.3: [26] A continuous function φ: $[0, \infty) \longmapsto \mathcal{R}^+$ is said to belong to Class $\mathcal{KR}$, $i.e.$, $\varphi \in \mathcal{KR}$ if (i) $\varphi(0) = 0$ (ii) φ is strictly increasing on $[0, \infty)$ (iii) $\lim_{r\to\infty}\varphi(r) = \infty$.

Note that $\varphi \in \mathcal{KR}$ implies that $\varphi \in \mathcal{K}$, but not the other way.

Lemma 4.4: [26] Assume that a system described by ordinary differential equations form

$$\dot{x} = f(t, x), \;\; x(t_0) = x_0$$

where $x \in \mathcal{R}^n$, f: $J \times B(r) \longmapsto \mathcal{R}$, $J = [t_0, \infty)$ and $B(r) = \{x \in \mathcal{R}^n \mid |x| < r\}$, possesses a unique solution $\forall x_0 \in \mathcal{R}^n$. If there exists a function $V(t, x)$ defined on $|x| \geq R_0$ (where R_0 may be large) and $t \in [0, \infty)$ with continuous first-order partial derivatives with respect to x, t and if $\exists\varphi_1, \varphi_2 \in \mathcal{KR}$ as defined in Definition 4.2 such that (1) $\varphi_1(|x|) \leq V(t, x) \leq \varphi_2(|x|)$; (2) $\dot{V}(t, x) \leq 0$ for all $|x| \geq R_0$ and $t \in [0, \infty)$, then the solutions of this system are uniformly bounded. In addition, if $\exists\varphi_2 \in \mathcal{K}$ as defined in

Definition 4.3 on $[0,\infty)$ as well as (3) $\dot{V}(t,x) \leq -\varphi_3(|x|)$, $\forall\, |x| \geq R_0$ and $t \in [0,\infty)$, then the solutions are uniformly ultimately bounded.

Then, we proceed to prove Theorem 4.1 in Section 4.3.

4.4.1 Proof of the Convergence

Proof: We consider the Lyapunov function candidate

$$V_1 \stackrel{\triangle}{=} \frac{1}{2} s^T s + \frac{1}{2\sigma}(a-\hat{a})^2. \tag{4.48}$$

The time-derivative of V_1 along s (4.24) and $\dot{s}$ (4.28) is deduced as

$$\begin{aligned} \dot{V}_1 &= s^T \dot{s} - \frac{1}{\sigma}(a-\hat{a})\dot{\hat{a}} \\ &= s^T [HR\Delta x + \Gamma(\cdot)] - \frac{1}{\sigma}(a-\hat{a})\dot{\hat{a}} \\ &= \underbrace{s^T HR\Delta x}_{W_1} + \underbrace{s^T \Gamma(\cdot)}_{W_2} - \underbrace{\frac{1}{\sigma}(a-\hat{a})\dot{\hat{a}}}_{W_3}. \end{aligned} \tag{4.49}$$

Now substituting the controller Δx (4.45) into W_1 of (4.49) leads to

$$W_1 = s^T HR\Delta x = -\frac{\rho_0 + \rho_t}{\alpha_0} s^T HRR^T H^T s. \tag{4.50}$$

Using α_0 in (4.43), we obtain

$$\begin{aligned} W_1 &= -\frac{\rho_0 + \rho_t}{\alpha_0} s^T Q s \\ &= -\frac{\rho_0 + \rho_t}{\alpha_0} \alpha_0 \left|\left|s\right|\right|^2 \\ &= -(\rho_0 + \rho_t) \left|\left|s\right|\right|^2. \end{aligned} \tag{4.51}$$

Substituting ρ_t (4.46) into modified W_1 (4.51) leads to

$$W_1 = -\rho_0 ||s||^2 - \frac{\hat{a}\mu^2}{\|s\| \mu + \varepsilon} ||s||^2 . \tag{4.52}$$

Similarly, W_2 can be conditioned by $||s||$ as

$$\begin{aligned} W_2 &= s^T \Gamma(\cdot) \\ &\leq \left|\left| s^T \Gamma(\cdot) \right|\right| \\ &\leq \left|\left| s^T \right|\right| ||\Gamma(\cdot)|| \leq a\mu ||s|| . \end{aligned} \tag{4.53}$$

In addition, applying $\dot{\hat{a}}$ (4.47) into W_3 leads to

$$\begin{aligned} W_3 &= \frac{1}{\sigma}(a - \hat{a})\dot{\hat{a}} \\ &= \frac{\kappa}{\sigma}(a - \hat{a})\hat{a} - (a - \hat{a})\frac{\|s\|^2 \mu^2}{\|s\| \mu + \varepsilon}. \end{aligned} \tag{4.54}$$

Combining W_1 in (4.52), W_2 in (4.53) and W_3 in (4.54), $\dot{V}_1$ in (4.49) turns to be

$$\begin{aligned} \dot{V}_1 \leq & -\rho_0 ||s||^2 - \frac{\hat{a}\mu^2}{\|s\| \mu + \varepsilon} ||s||^2 + \underbrace{a\mu ||s||}_{W_2'} \\ & + \underbrace{\frac{\kappa}{\sigma}(a - \hat{a})\hat{a}}_{W_4} - \underbrace{(a - \hat{a})\frac{\|s\|^2 \mu^2}{\|s\| \mu + \varepsilon}}_{W_5}. \end{aligned} \tag{4.55}$$

For the purpose of cancelling W_5 in (4.55), we rewrite $W_2^{'}$ as

$$\begin{aligned} W_2' &= ||s|| a\mu \frac{\|s\| \mu + \varepsilon}{\|s\| \mu + \varepsilon} \\ &= \frac{a\mu^2 \|s\|^2}{\|s\| \mu + \varepsilon} + \frac{a\varepsilon\mu \|s\|}{\|s\| \mu + \varepsilon}. \end{aligned} \tag{4.56}$$

Consequently, substituting W_2' (4.56) into $\dot{V}_1$ (4.55) leads to

$$\begin{aligned}\dot{V}_1 \;\leq\; & -\rho_0 \left|\left|s\right|\right|^2 \underbrace{-\frac{\hat{a}\mu^2}{\left\|s\right\|\mu+\varepsilon}\left|\left|s\right|\right|^2 + \frac{a\mu^2\left\|s\right\|^2}{\left\|s\right\|\mu+\varepsilon}}_{W_6} \\ & \underbrace{+\frac{a\varepsilon\mu\left\|s\right\|}{\left\|s\right\|\mu+\varepsilon}}_{W_7} + W_4 \underbrace{-(a-\hat{a})\frac{\left\|s\right\|^2\mu^2}{\left\|s\right\|\mu+\varepsilon}}_{W_5},\end{aligned} \tag{4.57}$$

it can be seen that

$$W_6 - W_5 = 0.$$

Therefore, $\dot{V}_1$ in (4.57) becomes

$$\dot{V}_1 \leq -\rho_0 \left|\left|s\right|\right|^2 + \underbrace{\frac{a\varepsilon\mu\left\|s\right\|}{\left\|s\right\|\mu+\varepsilon}}_{W_7} + \underbrace{\frac{\kappa}{\sigma}(a-\hat{a})\hat{a}}_{W_4}. \tag{4.58}$$

Since ε is a small positive constant, then

$$\frac{\left\|s\right\|\mu}{\left\|s\right\|\mu+\varepsilon} < 1$$

which leads to

$$W_7 \leq a\varepsilon. \tag{4.59}$$

Let us proceed to discuss W_4 in (4.55). On account of the identifies

$$\begin{aligned}(a-\hat{a})\hat{a} &= a\hat{a} - \hat{a}^2 \\ &= -\frac{1}{2}a^2 + a\hat{a} - \frac{1}{2}\hat{a}^2 + \frac{1}{2}a^2 - \frac{1}{2}\hat{a}^2 \\ &= -\frac{1}{2}(a-\hat{a})^2 + \frac{1}{2}a^2 - \frac{1}{2}\hat{a}^2 \\ &\leq -\frac{1}{2}(a-\hat{a})^2 + \frac{1}{2}a^2,\end{aligned}$$

we obtain

$$W_4 \leq -\frac{\kappa}{2\sigma}(a-\hat{a})^2 + \frac{\kappa a^2}{2\sigma}. \tag{4.60}$$

Finally, from $\dot{V}_1$ in (4.58), W_7 in (4.59) and W_4 in (4.60), we deduce that

$$\begin{aligned}
\dot{V}_1 &\leq -\rho_0 \left|\left|s\right|\right|^2 + a\varepsilon + -\frac{\kappa}{2\sigma}(a-\hat{a})^2 + \frac{\kappa a^2}{2\sigma} \\
&\leq -\rho_0 \left\|s\right\|^2 - \frac{\kappa}{2\sigma}(a-\hat{a})^2 + \frac{\kappa a^2}{2\sigma} + a\varepsilon \\
&\leq -\rho_0 s^T s - \frac{\kappa}{2\sigma}(a-\hat{a})^2 + \frac{\kappa a^2}{2\sigma} + a\varepsilon \\
&\leq -\varsigma V_1 + \frac{\kappa a^2}{2\sigma} + a\varepsilon,
\end{aligned} \tag{4.61}$$

where $\varsigma > 0$ and $\varsigma = \min\left\{2\rho_0,\ \kappa\right\}$, the confined $\dot{V}_1$ (4.61) implies that for $V_1 \geq V_{10} = \varsigma(\frac{\kappa a^2}{2\sigma} + a\varepsilon)$, $\dot{V}_1 \leq 0$. Therefore, according to Lemma 4.4, $s,\, \hat{a} \in \mathcal{L}_\infty$ which, together with $\mu \in \mathcal{L}_\infty$, implies that Δx, ρ_t and $\dot{\hat{a}} \in \mathcal{L}_\infty$ on the time interval $[0, T]$. In addition, we can establish by integrating $\dot{V}_1$ (4.61) that

$$\begin{aligned}
V_1 &= \frac{1}{2}s^T s + \frac{1}{2\sigma}(a-\hat{a})^2 \\
&\leq e^{-\varsigma t}V_{10} + \frac{\kappa a^2}{2\sigma} + a\varepsilon,
\end{aligned}$$

which implies that $(s, a-\hat{a})$ converges exponentially with a rate $e^{-\varsigma t}$ to a set containing origin:

$$D_1 = \left\{(s \in R,\ a-\hat{a} \in R) \mid V_{10} \leq d_1\right\}, \tag{4.62}$$

where $d_1 = \frac{\kappa a^2}{2\sigma} + a\varepsilon$.

4.4.2 Proof of the Boundedness of Tracking Errors

To restrict the bound set of the tracking errors e_1 and e_2, we first consider the Euclidean norm of s (4.24):

$$\begin{aligned} ||s||^2 &= s^T s \\ &= (e_1 + \eta e_2)^T (e_1 + \eta e_2) \\ &= ||e_1||^2 + \eta^2 ||e_2||^2 + 2\eta e_1^T e_2. \end{aligned} \tag{4.63}$$

In Chapter 3, we already clarified that there are two cases of equilibria (1) $b_l^* = 0$, $p_l^* = 0$, and (2) $b_l^* = 0$, $p_l^* > 0$. The tracking error boundedness will be studied based-on these two cases.

1. Assuming $b_l^d = 0$ and $p_l^d = 0$

From (4.23), if $b_l^d = 0$, then $e_{1l} = b_l - b_l^d \geq 0$ since $b_l \geq 0$. Similarly, if $p_l^d = 0$, then $e_{2l} = p_l - p_l^d \geq 0$ since $p_l \geq 0$. Hence, $e_1^T e_2 \geq 0$. Since s is bounded, then

$$2\eta e_1^T e_2 = ||s||^2 - ||e_1||^2 - \eta^2 ||e_2||^2 \tag{4.64}$$

is either bounded or negative if either e_1 or e_2 are unbounded, but the latter case is not acceptable because $e_1^T e_2 \geq 0$. Hence, e_1 and e_2 are bounded.

2. Assuming $b_l^d = 0$ and $p_l^d > 0$

If $p_l^d = a_0 > 0$ but a_0 is finite, since $e_{2l} = p_l - p_l^d$, we deduce that

$$-a_0 \leq e_{2l} \leq \infty,$$

note that $0 \leq e_{1l} \leq \infty$, then, $e_1^T e_2$ is either (a) bounded or (b) positive or (c) decrease towards $-\infty$ linearly. From $2\eta e_1^T e_2$ (4.64), if either $||e_1||$ or $||e_2||$ is unbounded, the right hand side (RHS) will decrease towards $-\infty$ quadratically, which contradicts the three possibilities (a), (b) and (c).

Therefore, the tracking error of backlog e_1 and link price e_2 are bounded in both cases. Since $(s, a - \hat{a})$ converges exponentially with a rate $e^{-\varsigma t}$ to a set containing the origin, $V_{10} \leq d_1 = \frac{\kappa a^2}{2\sigma} + a\varepsilon$ as in (4.62), then from the boundedness of $\dot{V}_1$ in (4.61), we deduce that

$$||s|| \leq \sqrt{\frac{\frac{\kappa a^2}{2\sigma} + a\varepsilon}{\varsigma}} = \sqrt{\frac{d_1}{\varsigma}},$$

where $\varsigma > 0$ and $\varsigma = \min\{2\rho_0,\ \kappa\}$ as defined in (4.61). From the Euclidean norm of $||s||^2$ in (4.63), it can be deduced that the tracking errors are constrained in the compact region

$$S = \left\{ e_1, e_2 \middle| \|e_1\| \leq ||s|| = \sqrt{\frac{d_1}{\varsigma}},\ \|e_2\| \leq \frac{||s||}{\eta} = \sqrt{\frac{d_1}{\eta^2 \varsigma}} \right\}, \tag{4.65}$$

which means that $\dot{V}_1 < 0$, if e_1, e_2 exceed the region of S in (4.65), then V_1 will strictly decrease, and consequently, e_1, e_2 and $(a - \hat{a})$ will decrease until the error states move back into the compact region of S.

4.5 Simulation Study

Next, we simulate the performance of our algorithm using the example network given in Section 2.2. The adaptation and robustness of the designed tracking control algorithm were investigated by adopting both constant and time-varying measured deterministic source accumulation rate. Note that the identical routing matrix

$$R = \begin{bmatrix} 1 & 0 & 1 & 0 & 0 & 0 & 0 & 0 & 0 & 0 \\ 0 & 1 & 0 & 1 & 0 & 0 & 0 & 0 & 0 & 0 \\ 0 & 0 & 0 & 0 & 1 & 0 & 0 & 0 & 0 & 0 \\ 0 & 0 & 0 & 1 & 1 & 0 & 0 & 0 & 0 & 0 \\ 0 & 0 & 0 & 1 & 1 & 0 & 0 & 0 & 0 & 0 \\ 0 & 0 & 0 & 0 & 0 & 1 & 0 & 0 & 0 & 0 \\ 0 & 1 & 0 & 0 & 0 & 0 & 0 & 0 & 0 & 0 \\ 0 & 0 & 0 & 0 & 0 & 0 & 0 & 1 & 0 & 0 \\ 1 & 0 & 0 & 0 & 1 & 0 & 1 & 0 & 0 & 0 \\ 0 & 0 & 0 & 0 & 0 & 1 & 0 & 0 & 0 & 0 \\ 0 & 1 & 0 & 0 & 0 & 0 & 0 & 1 & 0 & 0 \\ 0 & 0 & 0 & 0 & 0 & 0 & 0 & 0 & 1 & 0 \\ 0 & 1 & 0 & 0 & 0 & 0 & 0 & 1 & 0 & 1 \\ 0 & 0 & 0 & 0 & 0 & 0 & 0 & 0 & 0 & 0 \\ 1 & 0 & 0 & 0 & 1 & 1 & 1 & 0 & 1 & 0 \\ 1 & 0 & 0 & 0 & 0 & 0 & 1 & 0 & 1 & 0 \\ 0 & 1 & 0 & 0 & 0 & 0 & 0 & 1 & 0 & 1 \end{bmatrix}_{17\times 10}$$

was applied for all situations in this chapter.

4.5.1 Simulations for Constant Backbone Source Rate

Here, we assume that the link capacity c, the measured backbone source aggregate rate x_c, and the uncertainties are constant and chosen as

$$c_l = 100,\ x_{cl} = 50,\ \text{and}\ W_l = 15, \tag{4.66}$$

respectively. The network parameters are assigned as

$$\gamma = 0.2, \text{ and } \alpha = 0.01.$$

The control parameters are chosen as follows:

$$\varepsilon = 0.5,\ \eta = 0.01,\ \rho_0 = 0.002,\ \sigma = 0.6, \text{ and } \kappa = 1.6.$$

The initial conditions are set to be

$$\begin{aligned} \hat{a}(0) &= 4, \\ b_l(0) &= 0,\ p_l(0) = 0.2,\ s_l(0) = 0, \\ x(0) &= \begin{bmatrix} 20 & 20 & \cdots & 20 \end{bmatrix}^T_{1\times 10}, \\ y(0) &= Rx(0). \end{aligned}$$

The simulations are conducted under the two desired equilibria obtained in Chapter 3.

For the case of $b_l^d = 0$ *and* $p_l^d = 0$:

The tracking errors are defined as (4.23) in Section 4.2. Then, for this case, $e_1 = b$ and $e_2 = p$. From Figure 4.2, the tracking error performance shows how well the controller is able to track the desired backlog and link price. The performance of controller Δx, the sliding surface s, parameters $\hat{a}$ and ρ_t illustrates promising adaptation and robustness in Figure 4.3. Table 4.1 shows the tracking errors at the steady state. It is clear that the backlogs ended up at zero except for three bottleneck links l_{13}, l_{15} and l_{17}.

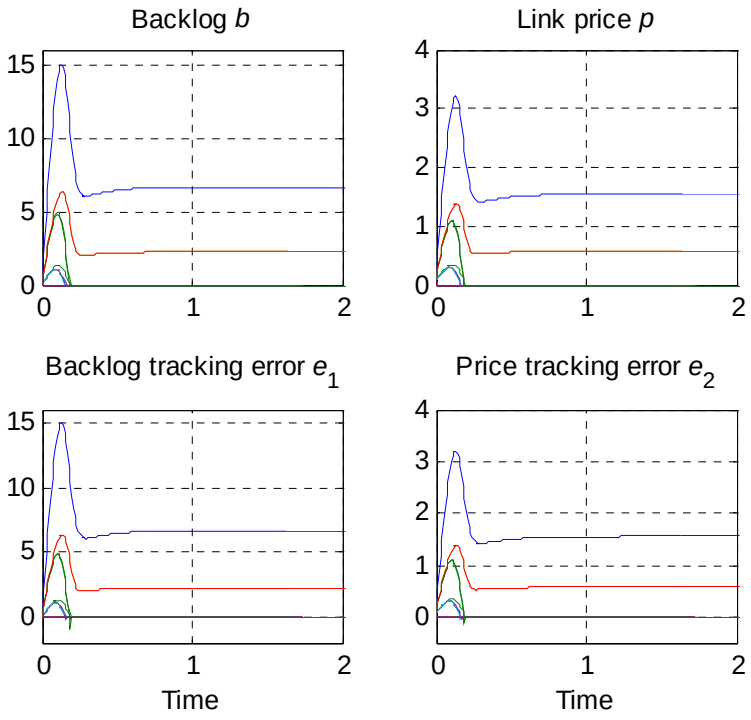

Figure 4.2. Tracking performance with x_{cl} at $b_l^d = 0$ and $p_l^d = 0$

Table 4.1. Steady state tracking errors as desired $b_l^d = 0$ and $p_l^d = 0$

	l_1	l_2	l_3	l_4	l_5	l_6
e_1	0	0	0	0	0	0
e_2	0	0	0	0	0	0
	l_7	l_8	l_9	l_{10}	l_{11}	l_{12}
e_1	0	0	0	0	0	0
e_2	0	0	0	0	0	0
	l_{13}	l_{14}	l_{15}	l_{16}	l_{17}	
e_1	2.2517	0	6.6765	0	2.2517	
e_2	0.6612	0	1.8036	0	0.6612	

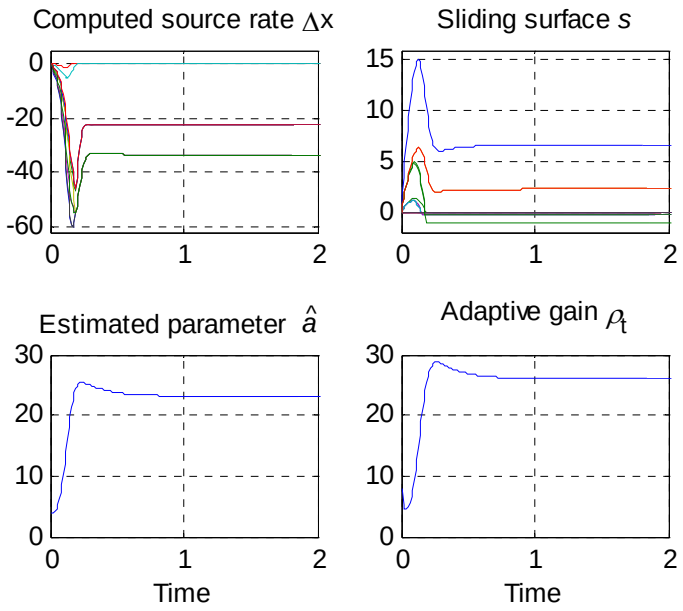

Figure 4.3. Control performance with x_{cl} at $b_l^d = 0$ and $p_l^d = 0$

For the case of $b_l^d > 0$ and $p_l^d > 0$:

According to the definition of sliding surface s in (4.24) of Section 4.2, the tracking error e_1 is the main effective element reflecting s, which was indicated in Figure 4.4. The trajectories of backlog and link price, as well as the link aggregate rate y are shown in Figure 4.5. Clearly, the settling is not reached as quickly as in Figure 4.3. Table 4.2 slightly differs from Table 4.1 because of the positive b_l^d and p_l^d. However, the tracking errors are still bounded and stability is maintained.

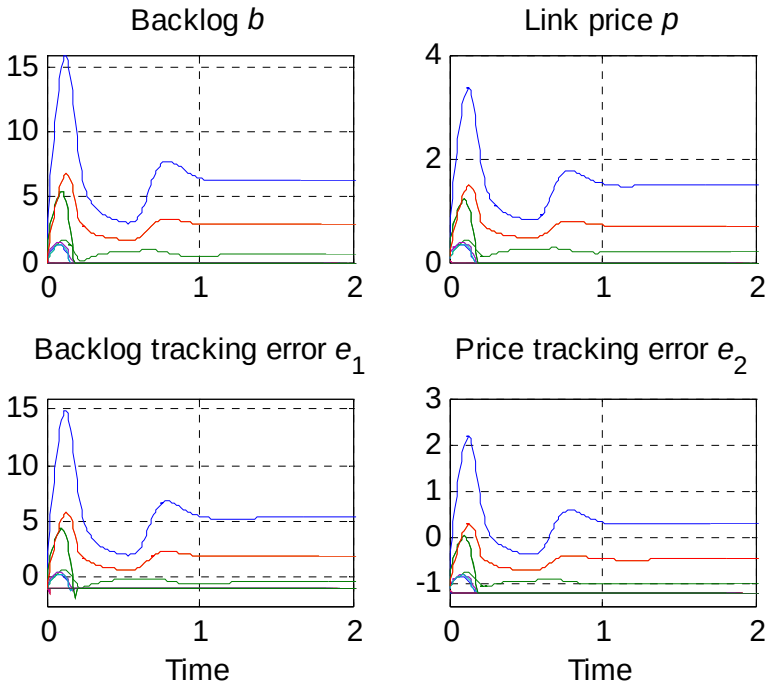

Figure 4.4. Tracking performance with x_{cl} at $b_l^d > 0$ and $p_l^d > 0$

Table 4.2. Steady state tracking errors as desired $b_l^d > 0$ and $p_l^d > 0$

	l_1	l_2	l_3	l_4	l_5	l_6
e_1	-1.0000	-0.4388	-1.0000	-1.0000	- 1.0000	- 1.0000
e_2	-1.2001	-0.9851	-1.2001	-1.2001	-1.2001	-1.2001
	l_7	l_8	l_9	l_{10}	l_{11}	l_{12}
e_1	- 1.0000	- 1.0000	- 1.0000	- 1.0000	- 1.0000	- 1.0000
e_2	-1.2001	-1.2001	-1.2001	-1.2001	-1.2001	-1.2001
	l_{13}	l_{14}	l_{15}	l_{16}	l_{17}	
e_1	1.8719	- 1.0000	5.3221	- 1.0000	1.8719	
e_2	-0.3907	-1.2001	0.5178	-1.2001	-0.3907	

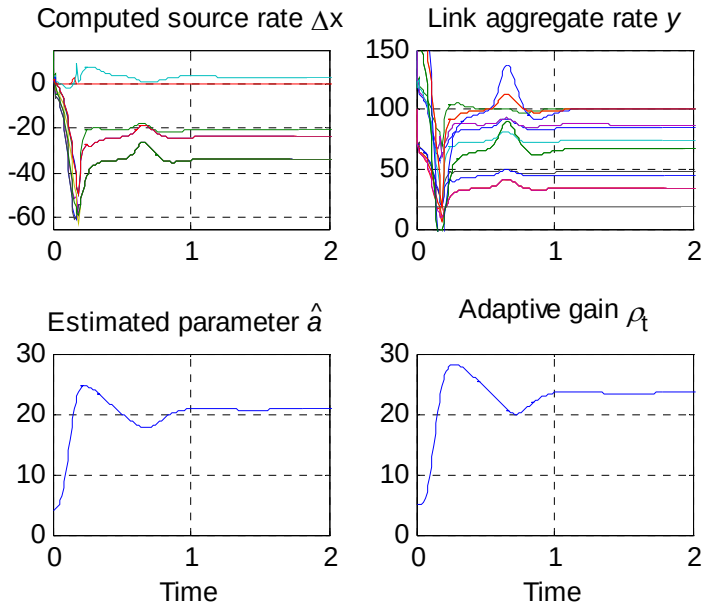

Figure 4.5. Control performance with x_{cl} at $b_l^d > 0$ and $p_l^d > 0$

Remark: From the simulations of both cases, we can see that 1) the links l_{13}, l_{15} and l_{17} are congested in both cases due to at least three routes passing along these links. The congestion is signaled by the buildup of a backlog at the bottleneck, and the propagation delays become significant; 2) since there are five routes assigned along link l_{15}, the congestion of this bottleneck is more severe than that of links l_{13} and l_{17}, but there is no backlog in l_{16}; 3) l_{14} is an idle link in this network, l_{13} and l_{17} are in the same congestion situation.

4.5.2 Simulations for Time-Varying Backbone Source Rate

An important aspect of various networks is their dynamic behavior. Next, we considered the case where the measured backbone source aggregate rate is time varying:

$$x_{cl}(t) = 10 + \max\left\{0,\ 40\sin(\pi(t-5)/6)\right\}, \tag{4.67}$$

The profile of control input x_{cl} is shown in Figure 4.6. The other network parameters, initial conditions and control parameters are set same as that in Subsection 4.5.1.

For the case of $b_l^d = 0$ *and* $p_l^d = 0$:

Figure 4.7 gives the trajectory of the adaptive gain ρ_t and the estimated parameter $\hat{a}$. There are slight overshoots in the trajectory of tracking errors e_1, e_2, and demanded link aggregate rate y shown in Figure 4.6 and Figure 4.7, owing to the severe congestion on bottleneck link l_{15}. However, the steady state is reached in a short time.

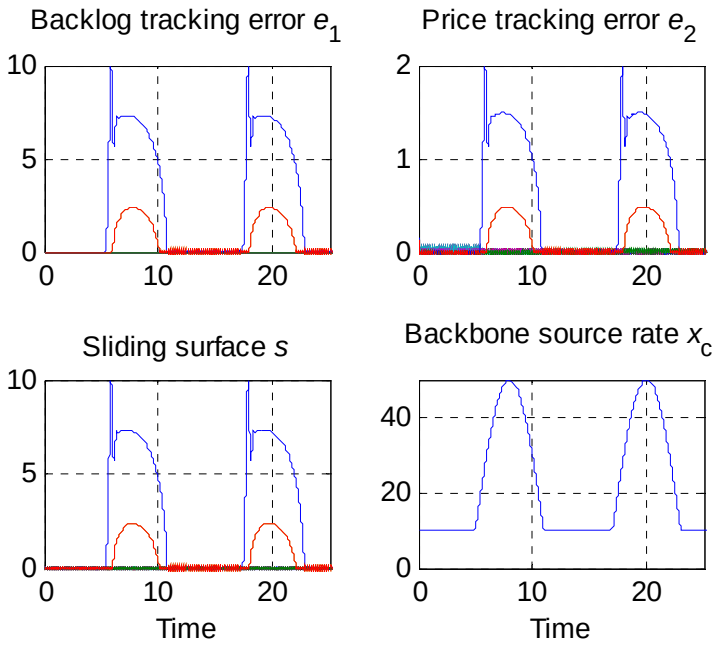

Figure 4.6. Tracking performance with $x_{cl}(t)$ at $b_l^d = 0$ and $p_l^d = 0$

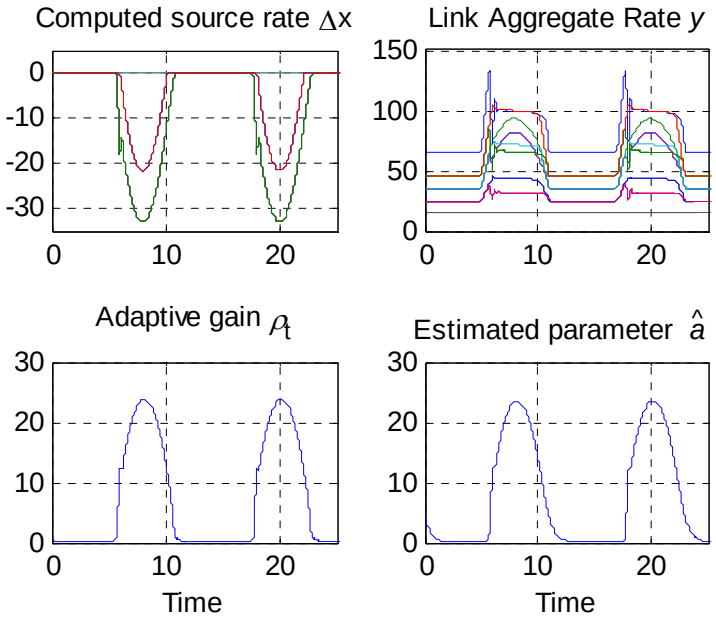

Figure 4.7. Control performance with $x_{cl}(t)$ at $b_l^d = 0$ and $p_l^d = 0$

For the case of $b_l^d > 0$ *and* $p_l^d > 0$:

Figure 4.8 also shows very promising tracking performance with Δx taking stronger control actions, and that asymptotic stability is maintained with respect to challenging positive desired b_l^d and b_l^d.

Therefore, we can conclude that, under the assumptions of bounded constant disturbances and uncertainties, the designed control scheme is effective and able to ensure stability on the dynamic network source aggregate rate.

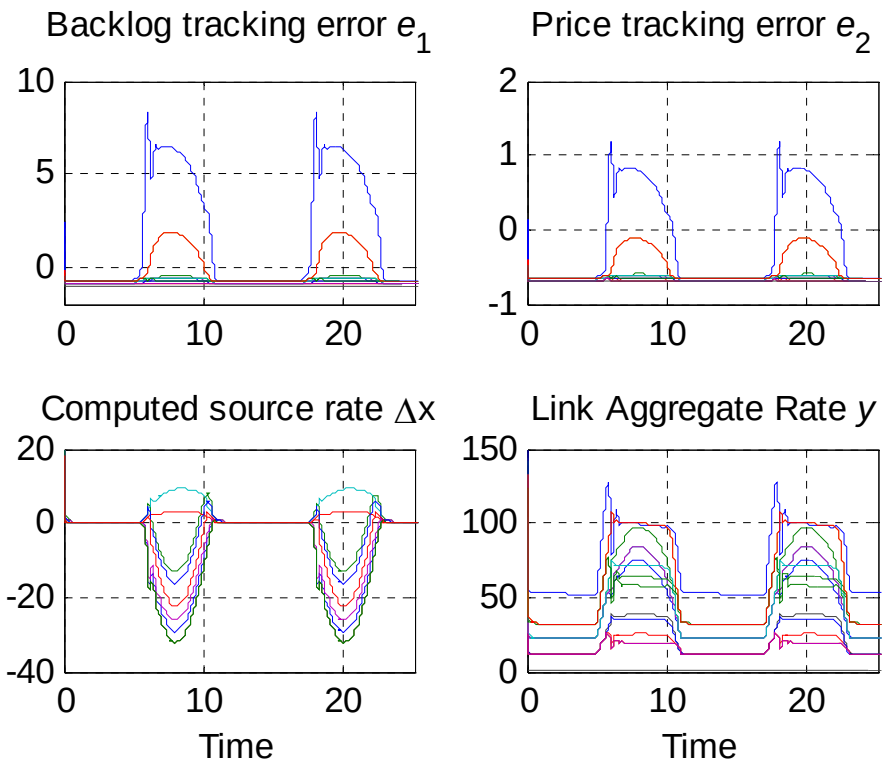

Figure 4.8. Performance of e_1, e_2 Δx **and** y **with** $x_{cl}(t)$ **at** $b_l^d > 0$ **and** $p_l^d > 0$

CHAPTER 5
EFFECTS OF UNCERTAINTIES AND DISTURBANCES

Adaptation represents the ability of the network to respond to varying conditions. This chapter investigates the effectiveness and adaptation of the proposed control scheme in terms of counteracting the effect of uncertainties and disturbances from unknown local traffic or from outside of the controlled network.

5.1 Effect of Uncertainties

We postulate an uncertainty Γ in (4.37) of Section 4.2 that is dynamic and depends on the system state b as

$$\Gamma = \frac{(Fb) \diamond b}{||b||} \tag{5.1}$$

where F is a matrix randomly generated in the simulations, the initial backlog b is also randomly chosen between $[0, 1]$, and ($\diamond$) denotes element-wise multiplication. Here, with the same control parameters set in Chapter 4, we only discuss the case of $b_l^d > 0$ and $p_l^d > 0$. Comparing with Figure 4.8, at least one link of the controlled network resulted in an increase of tracking errors e_1, e_2 as well as backlog b and travelling cost p in Figure 5.1, due to the influence of uncertainty Γ. We see that although the controller Δx needed more time to "learn" how to control the source aggregate rate, the steady state was reached in a short time as shown in Figure 5.2. The controller is apparently able to stabilize the system.

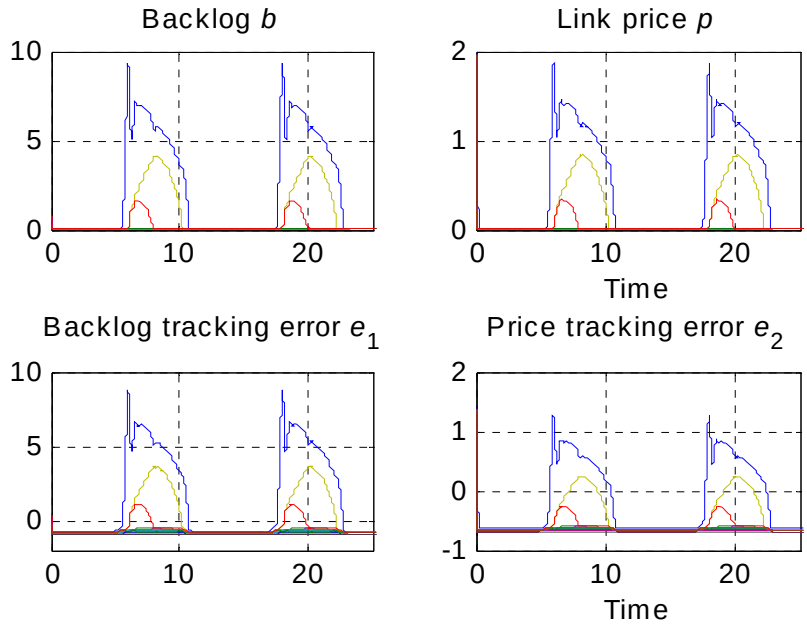

Figure 5.1. Tracking performance with $x_{cl}(t)$ and elastic uncertainty Γ

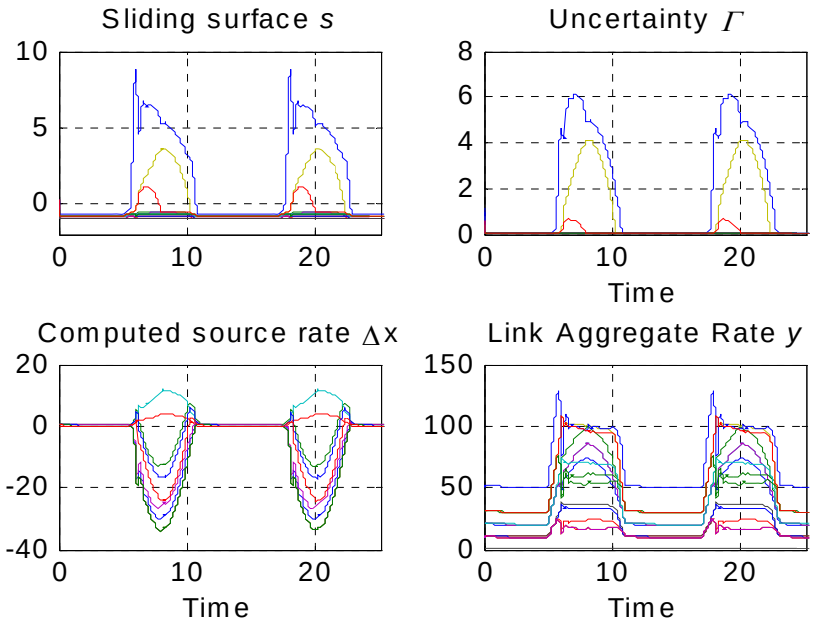

Figure 5.2. Control performance with $x_{cl}(t)$ and elastic uncertainty Γ

5.2 Effect of Random Disturbances

We assume the disturbance W defined in (4.25) of Section 4.2 is dynamic instead of constant, which was investigated in subsection 4.5.1 and subsection 4.5.2. Without loss of generality, we assume W is random but low-frequency and bounded within the link capacity c, $i.e.$ $W(t) \in [0, c]$ for $\forall t$. The simulations are conducted under the conditions $b_l^d > 0$ and $p_l^d > 0$.

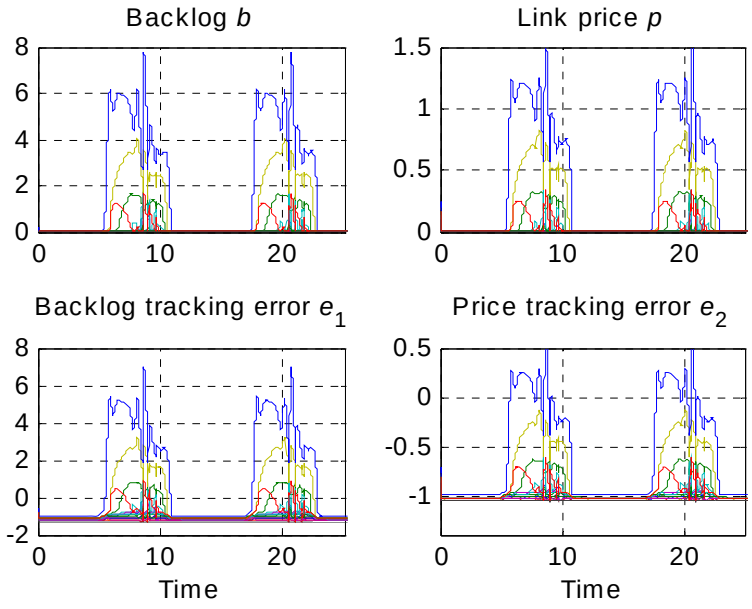

Figure 5.3. Tracking performance with random disturbance W at $b_l^d > 0$ and $p_l^d > 0$

As can be seen in Figure 5.3 and Figure 5.4, the performance of tracking errors and controller with random disturbances W involves severe unwanted chattering. The chattering usually exists in normal sliding mode control, due to switching actuations responding to sensitive compensating units. Therefore, additional measures are needed to eliminate the chattering problem and at the same time maintain asymptotic stability.

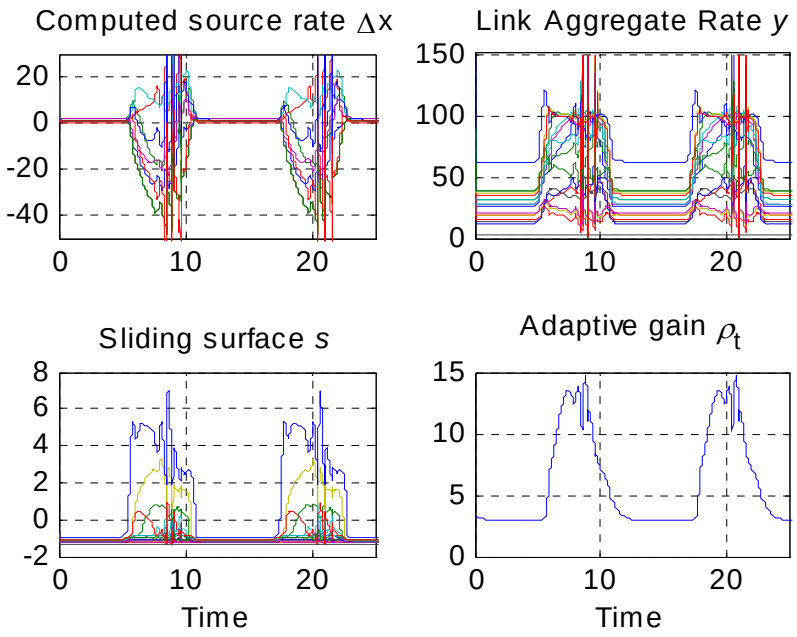

Figure 5.4. Control performance with random disturbance W at $b_l^d > 0$ and $p_l^d > 0$

5.2.1 Adding a dead zone

Considering the controller Δx (4.45), we denote

$$g = R^T H^T s, \tag{5.2}$$

where $g \in \mathcal{R}^k$, by introducing a dead-zone vector such that

$$\bar{g}_k = \begin{cases} 0 & \text{if } |g_k| \leq \xi \\ g_k - \xi & \text{if } g_k > \xi \\ g_k + \xi & \text{if } g_k < -\xi \end{cases}, \tag{5.3}$$

where ξ is a small positive number. We choose time step $\Delta T = 0.01$, and the dead zone weight of Δx is $\xi = 3.6$. Figure 5.5 shows the chattering-free adaptation of the resulting algorithm, and the controller needs more actions to stabilize the system.

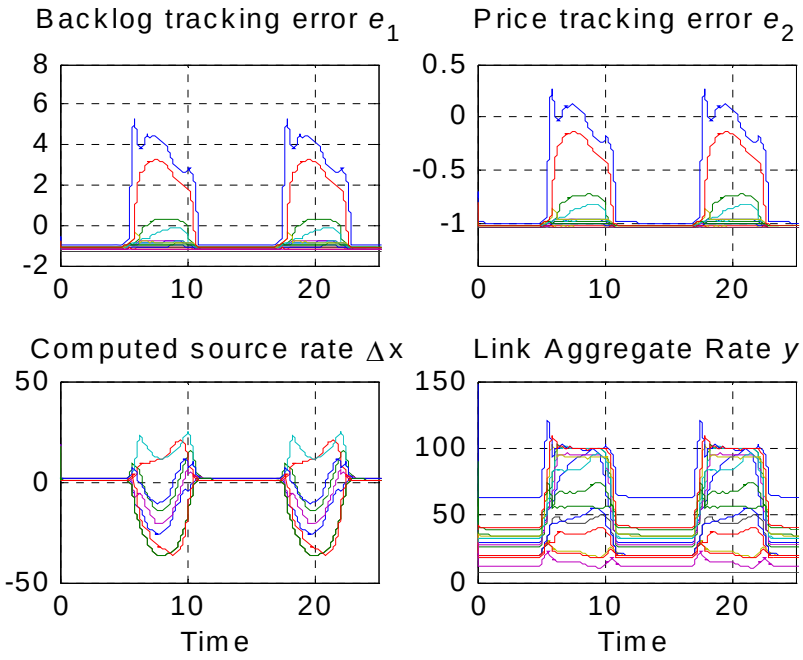

Figure 5.5. Tracking and control performance with random W at $b^d > 0$ and $p^d > 0$

5.3 Conclusions

With the promising simulations illustrated in the precede Sections, we can conclude that the uncertain local traffic and external disturbances can be effectively handled without sacrificing the robustness and stability.

CHAPTER 6
SIMULATIONS IN A SMALL WORLD NETWORK

This chapter investigates the adaptation and robustness of the control law proposed in Chapter 4 to more general such as small-world networks. The topology of a small-world network is obtained by random rewiring a regular network, typically a lattice. The random rewiring typically changes the average path length and the clustering coefficient favorably. The salient features of this system lie in high clustering of the nodes, like regular lattices, yet having small characteristic path lengths, like random graphs [29].

6.1 Property of the Small World Network

The small-world phenomenon is a feature of many complex networks in which any two arbitrary nodes can be connected by a path of a few links. This means that the average distance between two nodes (i.e. characteristic length) is relatively small in small-world networks.

A small world network can contain cliques, and near-cliques, meaning sub-networks which have connections between almost any two nodes within them. Therefore, most pairs of nodes will be connected by at least one short path. We denote the average node degree by k_1, and the probability of random rewiring as ρ. The random rewiring procedure for interpolating a regular original lattice is illustrated in Figure 6.1. Two other instances of small world networks are shown in Figure 6.2 and Figure 6.3. Note that the construction does not alter the number of vertices or edges in the graph. With a rewiring probability,

an edge will be rewired to a vertex chosen uniformly at random over the entire graph, with duplicate edges forbidden; otherwise the edge will be left in place.

Models of dynamic systems possessing the small-world property have enhanced signal propagation speed, computational power, and synchronizability. In particular, infectious diseases spread more easily in small-world networks than in regular lattices.

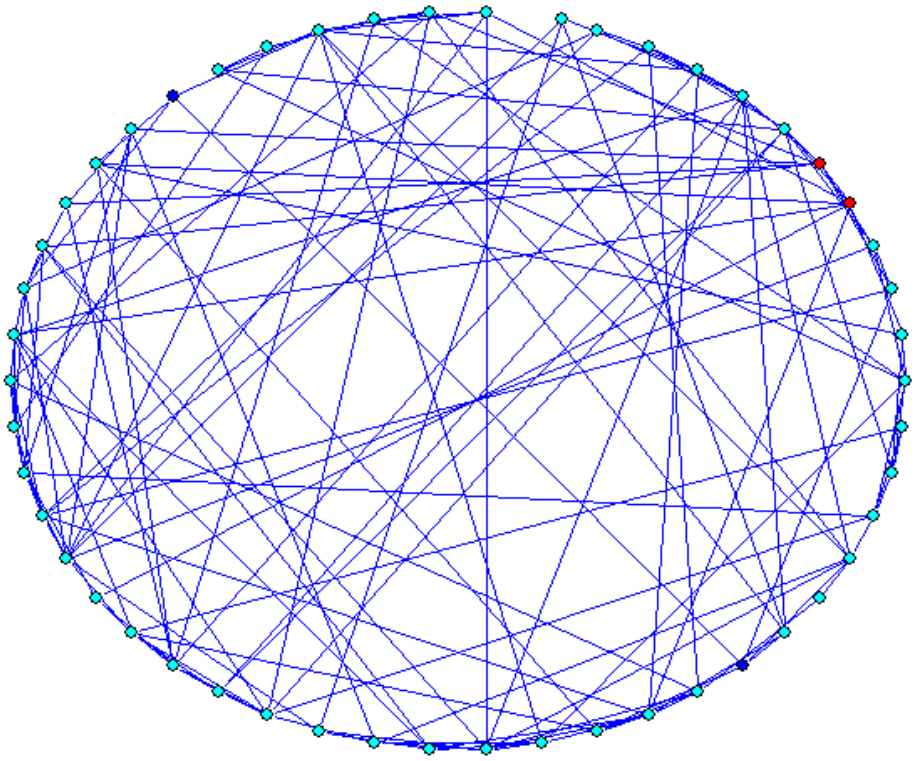

Figure 6.1. Small world network with 50 nodes as $k_1 = 3, \rho = 0.5$

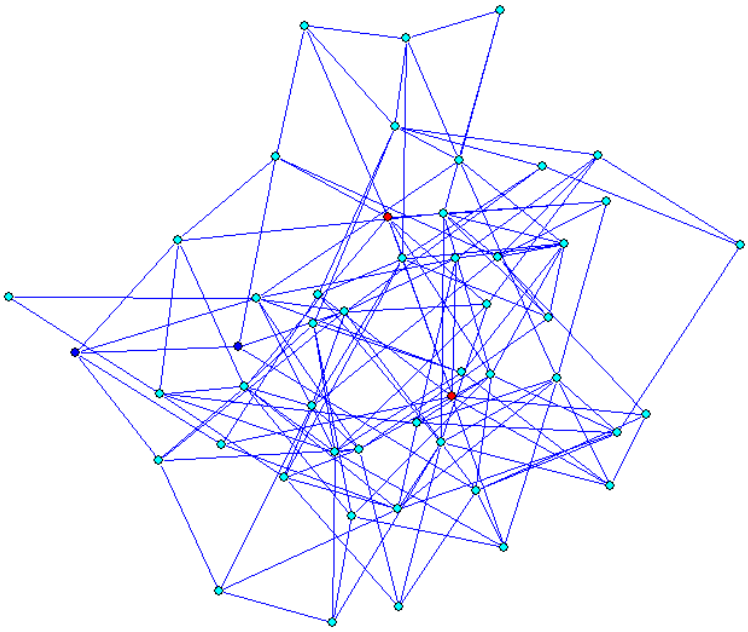

Figure 6.2. Small world network with 50 nodes as $k_1 = 3$, $\rho = 0.5$ in free 2-D

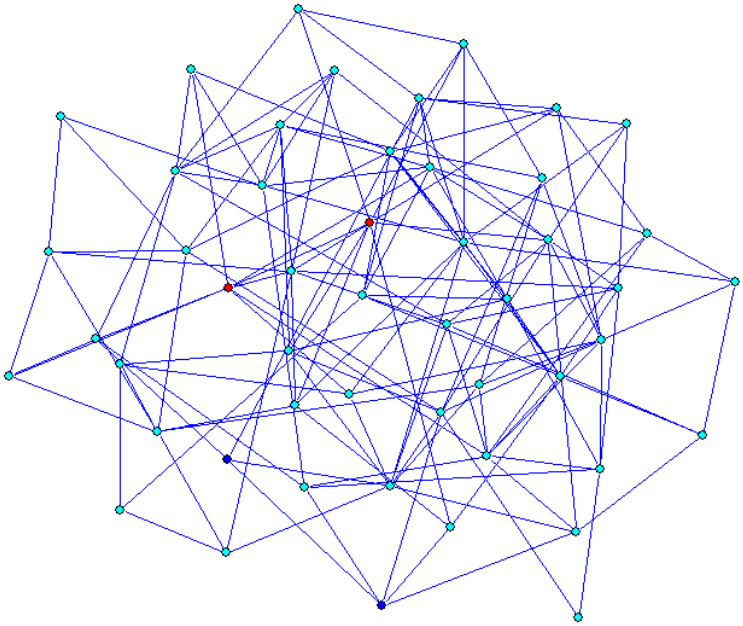

Figure 6.3. A random small world network with 50 nodes as $k_1 = 3$, $\rho = 0.5$

6.2 Small World Network Case Study

6.2.1 Generating the Routing Matrix

Assume the number of nodes in a small world network is 50, from which we randomly choose 20 Origin-Destination (OD) pairs. These OD pairs are obtained by randomly choosing origin nodes and destination nodes from 50 nodes. Note that there are multiple paths for each OD pair, many of which can be disjoint. The three shortest disjoint paths will be chosen for each OD pair. Since the number of disjoint paths of some OD pairs might be less than 3, the sum of disjoint paths will not exceed 60. The method to specify a routing matrix for the simulation is illustrated in Figure 6.4.

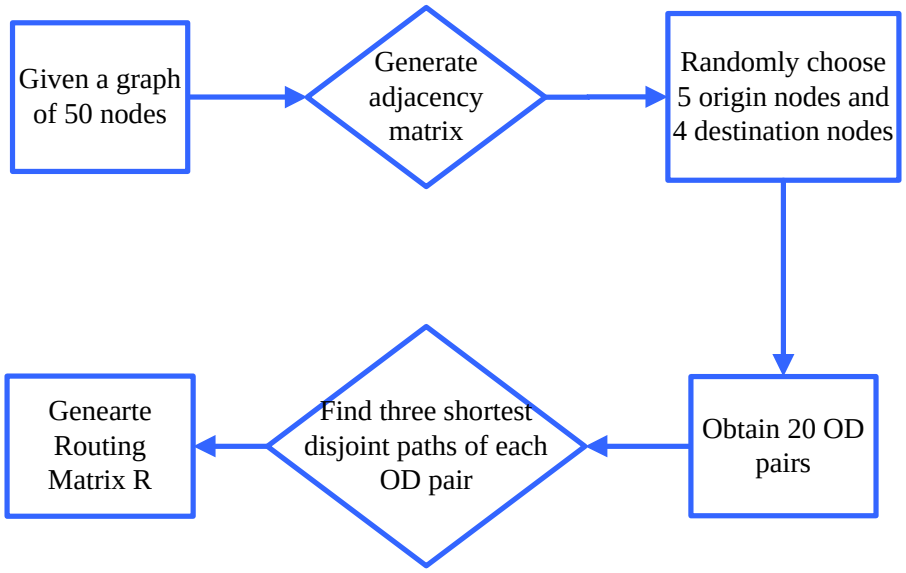

Figure 6.4. Flow chart of obtaining the routing matrix from a small world network

Because of the randomness of choosing the origin and destination nodes, the generated OD pairs are different for each simulation run. Hence the routing matrix is also different for each run. Subsequently, the image of routing matrix will show the links used by the

disjoint paths under considered. We investigate the performance of the control algorithm of the small-world network by considering different node degree k_1 and rewiring probability ρ.

6.2.2 Simulations for Constant Backbone Source Rate x_c

The control parameters and initial conditions are chosen same as those in Section 4.5.

For the case of $b_l^d = 0$ *and* $p_l^d = 0$:

Figure 6.6 illustrates the tracks of backlogs and link prices for the routing matrix in Figure 6.5 as well as the corresponding errors. It can be seen from Figure 6.7 that the system reaches the steady state in a short time. Δx is the adaptive control algorithms proposed in Chapter 4. The adaptive gain ρ_t and the estimated parameter $\hat{a}$ converge to constant in the steady-state.

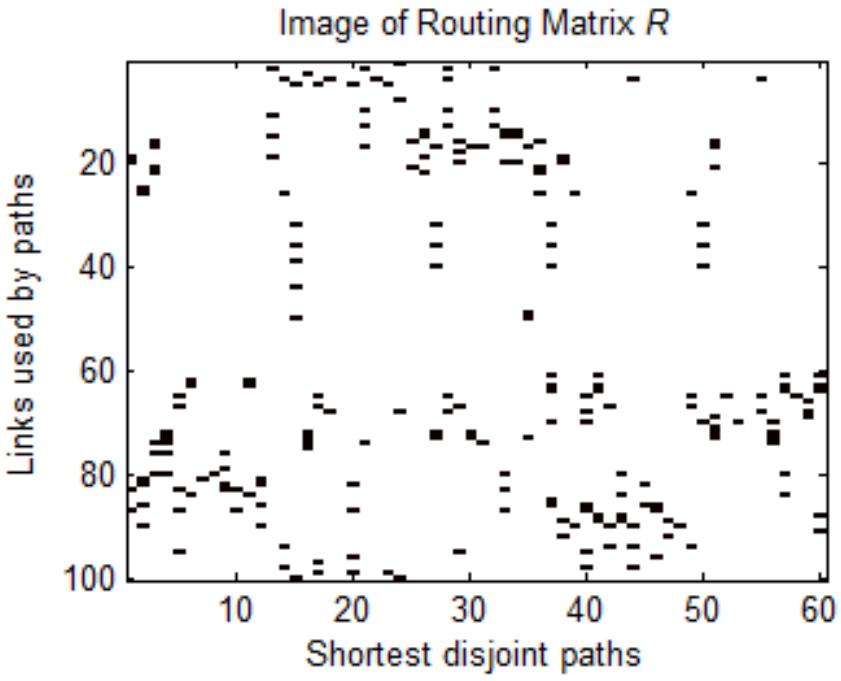

Figure 6.5. Routing Matrix $R(100, 60)$ **with** x_{cl} **as** $b_l^d = p_l^d = 0$, $k_1 = 2$ **and** $\rho = 0.3$

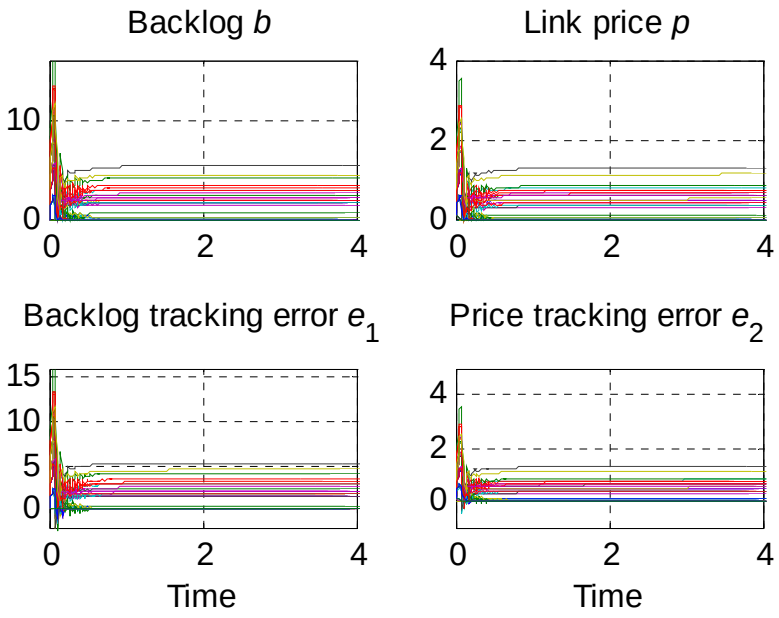

Figure 6.6. Tracking performance with x_{cl} as $b_l^d = p_l^d = 0$, $k_1 = 2$ and $\rho = 0.3$

For the case of $b_l^d > 0$ and $p_l^d > 0$:

For this simulation we will choose the desired network states

$$b_l^d = 0.8, \tag{6.1}$$

$$p_l^d = 0.9, \tag{6.2}$$

$$\dot{p}_l^d = 0.01. \tag{6.3}$$

Please note that at this condition, the desired states (6.1) and (6.2) are not the allowable equilibrium states as specified in Chapter 3.

Figure 6.8 shows an example of routing matrix with $k_1 = 4$ and $\rho = 0.5$. Although the positive desired network dynamics b_l^d and p_l^d are not equilibrium points, the controller

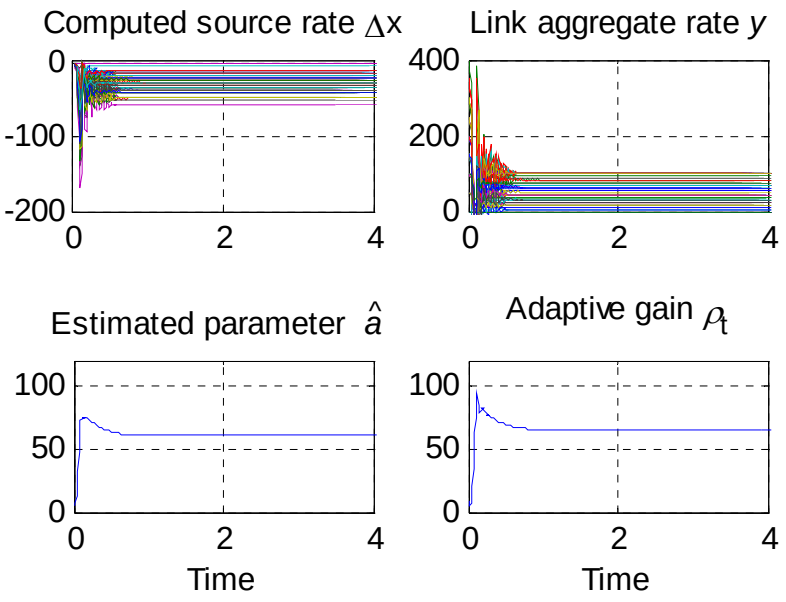

Figure 6.7. Control performance with x_{cl} as $b_l^d = p_l^d = 0$, $k_1 = 2$ and $\rho = 0.3$

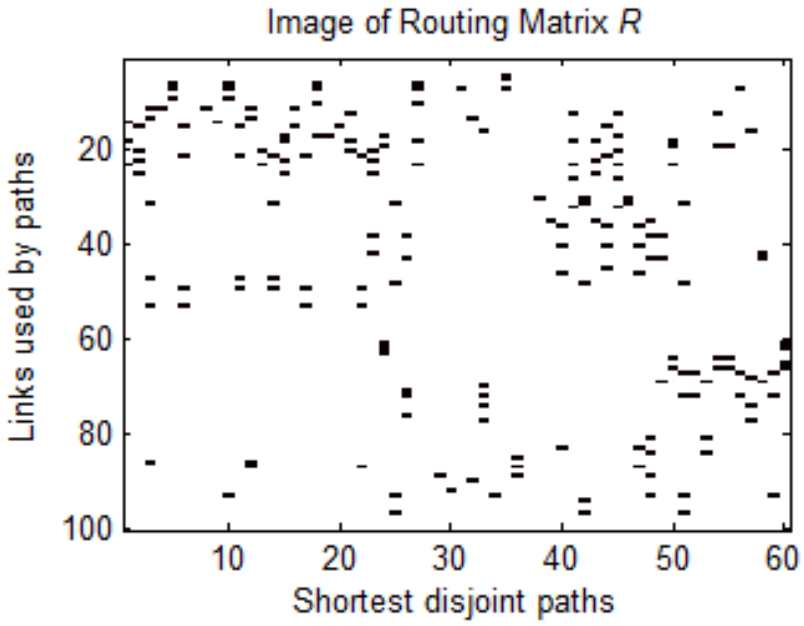

Figure 6.8. $R(100, 60)$ **with** x_{cl} **at** $b^d > 0, p^d > 0, k_1 = 4$ **and** $\rho = 0.5$

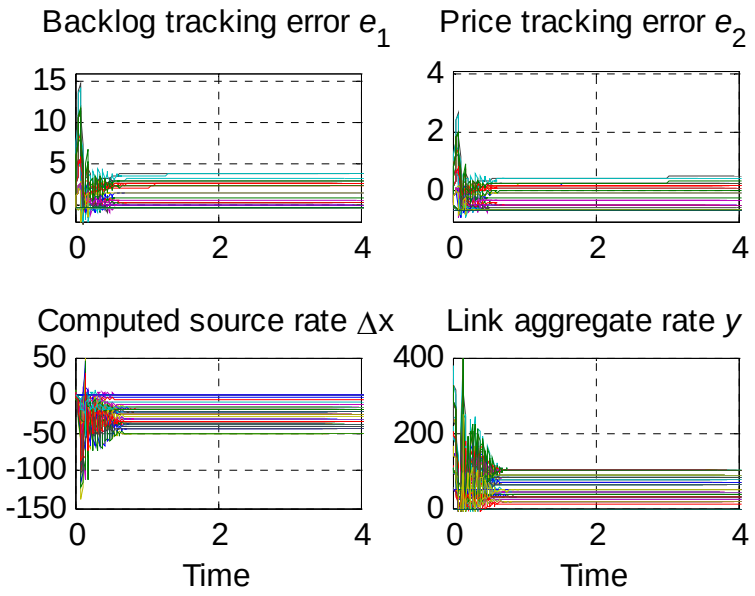

Figure 6.9. Tracking and control performance at $b^d > 0, p^d > 0, k_1 = 4$ and $\rho = 0.5$

still achieved reasonable tracking precision and robust stability in Figure 6.9. However, comparing this case to the case of $b_l^d = 0$ and $p_l^d = 0$, the controller needs more time to stabilize the network flow.

6.2.3 Simulations for Time-Varying Backbone Source Rate x_c

Next, we considering the case of a time-varying backbone source rate. For simplicity, we assume the same profile of x_c in equation (4.67).

For the case of $b_l^d = 0$ and $p_l^d = 0$:

Figure 6.10 shows an example of the routing matrix with $k_1 = 5$ and $\rho = 0.7$. The controller Δx responded effectively in adapting to the variation pace of the backbone source rate x_c and stabilized the system in a very short time. The tracking errors e_1 and e_2 and the aggregate rate y are bounded as shown in Figure 6.11.

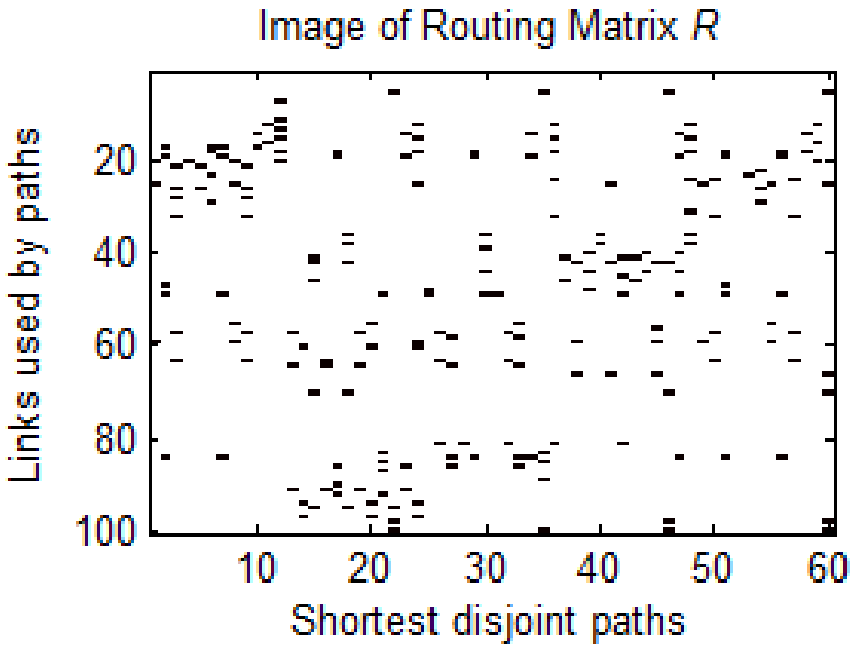

Figure 6.10. $R(100, 60)$ **with** $x_{cl}(t)$ **at** $b^d = p^d = 0$, $k_1 = 5$ **and** $\rho = 0.7$

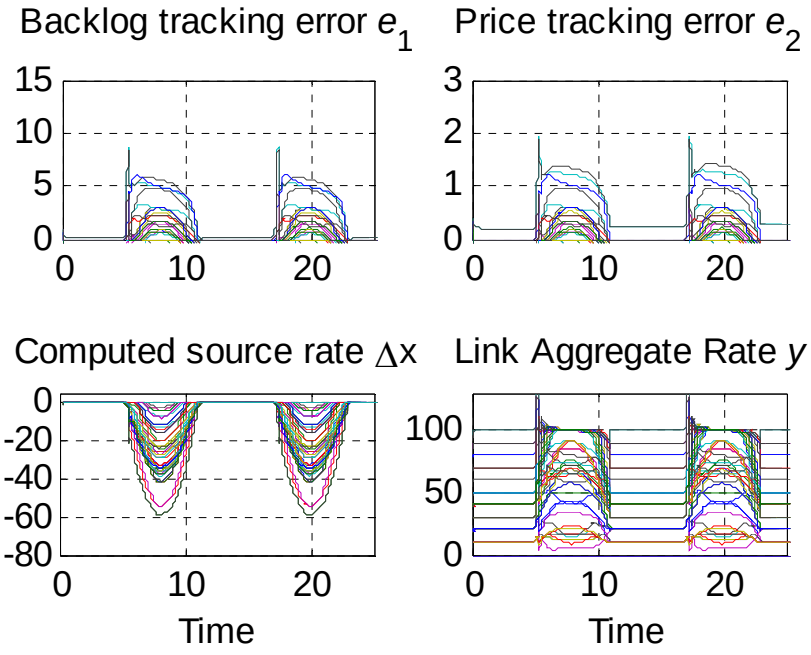

Figure 6.11. Tracking and control performance as $b^d = p^d = 0$, $k_1 = 5$ **and** $\rho = 0.7$

For the case of $b_l^d > 0$ *and* $p_l^d > 0$:

Here, we conduct the simulations by choosing the desired network dynamics as

$$\begin{aligned} b_l^d &= 0.5, \\ p_l^d &= 0.6, \\ \dot{p}_l^d &= 0.01. \end{aligned}$$

For this case, as well, the time-varying backbone source rate x_c will increase the difficulty of controlling the flow tracking error. The routing matrix in Figure 6.12 is obtained by setting $k_1 = 3$ and $\rho = 0.5$. Since the interactions between some links of the heterogeneous small-world network are highly clustered and disordered, it will be harder for the controller to attain steady controlling and precise tracking. In fact, although the controller Δx in Figure 6.13 acts vigorously, the link aggregate rate y is large but bounded. The control results show that additional rerouting methods are needed to reduce the congestion when there are too many overlaps of the shortest disjoint paths that chosen by each OD pair.

Figure 6.14 is obtained by increasing the node degree and link rewiring probability to $k_1 = 5$ and $\rho = 0.8$, the tracking and control performance shown in Figure 6.15 are acceptable. The controller achieves robust tracking at both peak usage intervals and in low-usage intervals of the source aggregate rate x_c.

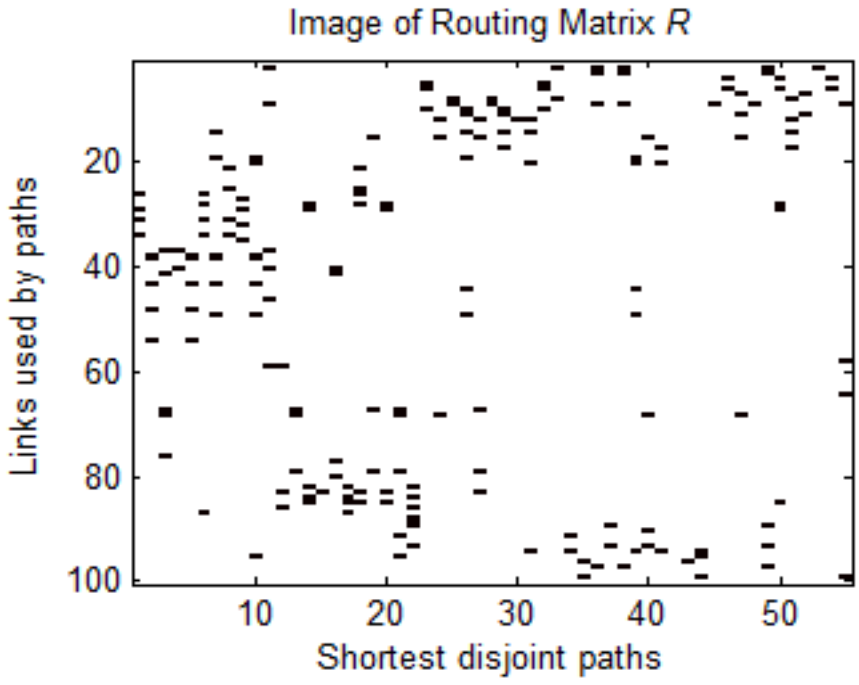

Figure 6.12. $R(100, 56)$ **with** $x_{cl}(t)$ **as** $b^d > 0, p^d > 0, k_1 = 3$ **and** $\rho = 0.5$

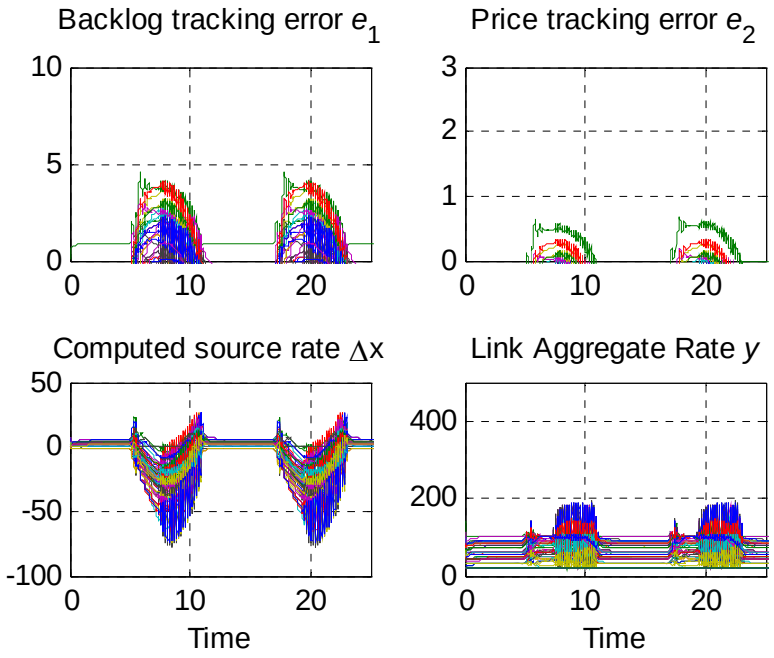

Figure 6.13. Tracking and control performance as $b^d > 0, p^d > 0, k_1 = 3$ **and** $\rho = 0.5$

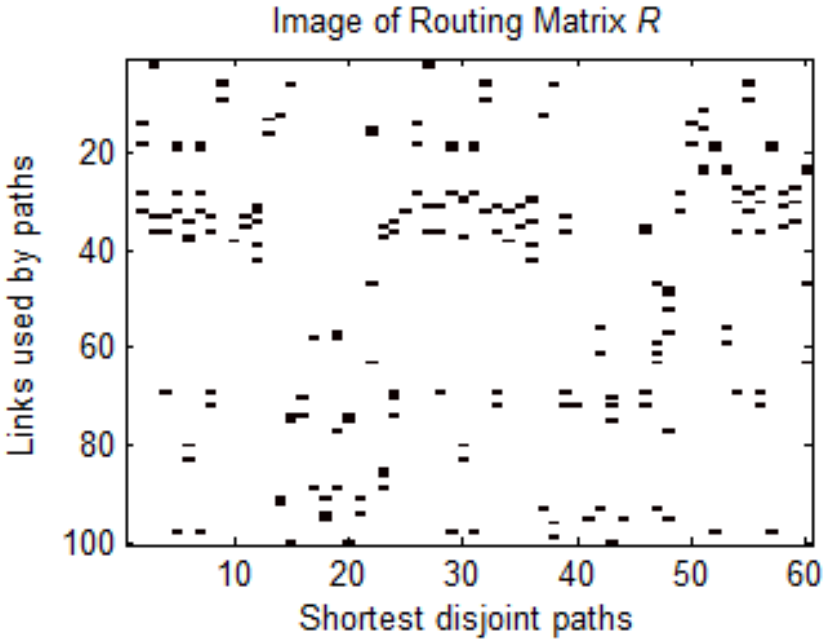

Figure 6.14. $R(100, 60)$ **with** $x_{cl}(t)$ **as** $b^d > 0$, $p^d > 0$, $k_1 = 5$ **and** $\rho = 0.8$

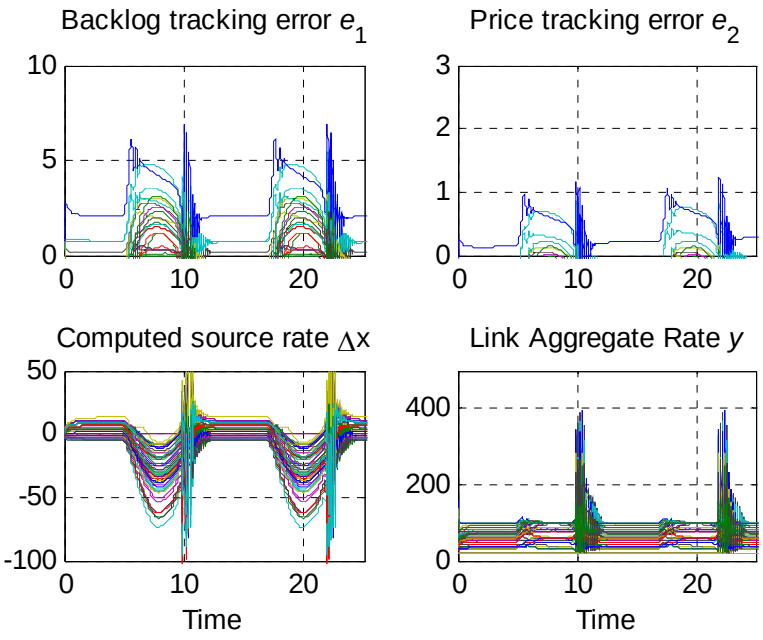

Figure 6.15. Tracking and control performance as $b^d > 0$, $p^d > 0$, $k_1 = 5$ **and** $\rho = 0.8$

For the case of $b_l^d = 0$ *and* $p_l^d > 0$:

Note that this case is an allowable equilibrium condition as stated in Chapter 3. The simulations are conducted by choosing the desired network dynamics as

$$\begin{aligned} b_l^d &= 0, \\ p_l^d &= 0.6, \\ \dot{p}_l^d &= 0.01. \end{aligned}$$

Figure 6.16 is a routing matrix generated by setting $k_1 = 4$ and $\rho = 0.8$. Figure 6.17 shows terrific tracking performance of the desired link prices, as well as the high control efficiency and strong adaptation to the source rate propagation of the proposed control algorithms.

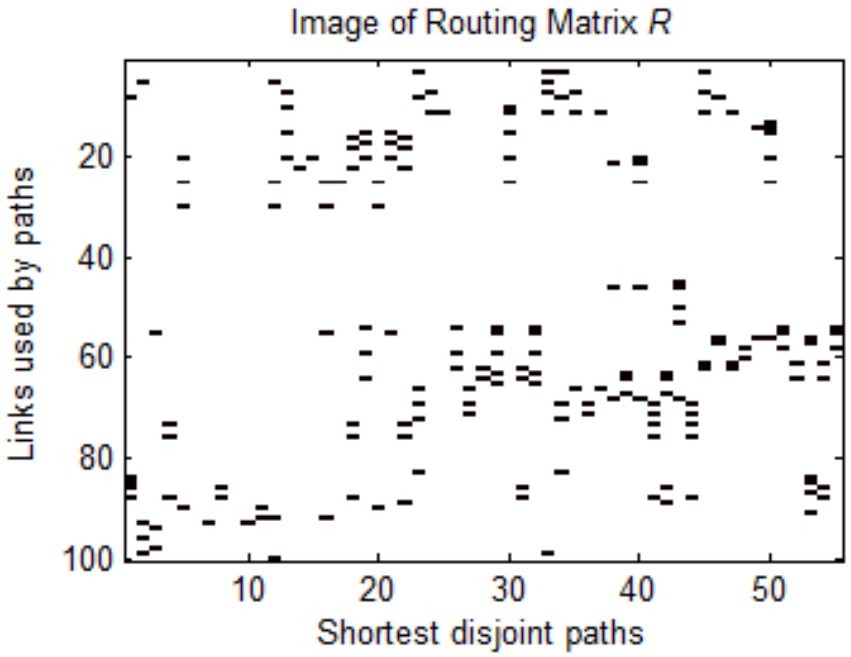

Figure 6.16. $R(100, 60)$ **with** $x_{cl}(t)$ **as** $b^d = 0$, $p^d > 0$, $k_1 = 4$ **and** $\rho = 0.8$

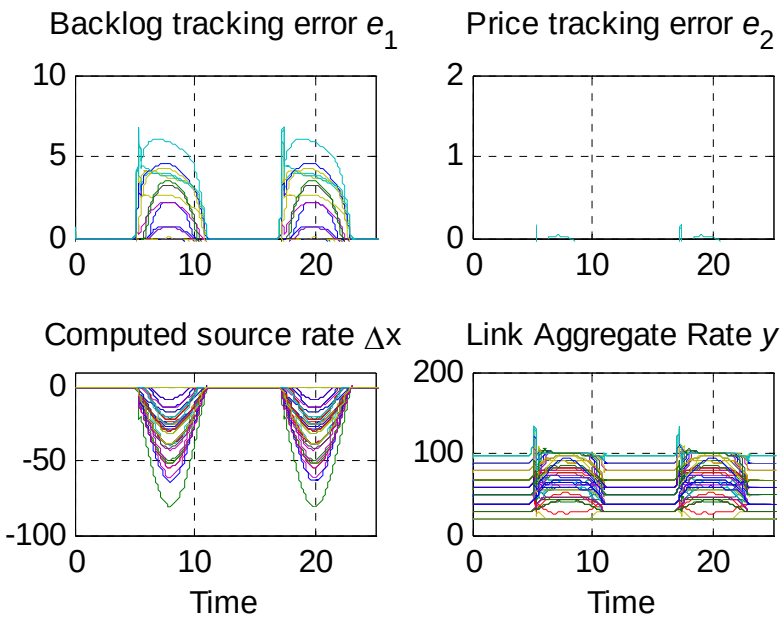

Figure 6.17. Tracking and control performance as $b^d = 0, p^d > 0, k_1 = 4$ and $\rho = 0.8$

6.2.4 Statistics analysis of the rewiring probability

To study the influence of the rewiring probability on the tracking errors, we performed a statistical analysis of simulation results. For each rewiring probability ρ, generate 20 small world networks and we record the average values of the tracking errors. Please note that the tracking errors considered are from the latter 30% of the simulation time, which lies into the time interval of the steady state.

We studied the network as the case of $b_l^d > 0$ and $p_l^d > 0$, as well as of $b_l^d = 0$ and $p_l^d = 0$. For simplicity, we utilize the same profile of x_c in equation (4.67). The relationship between the rewiring probability and the average errors of all the links is shown in the Table 6.1, Figure 6.18 and Figure 6.19.

Table 6.1. The average tracking errors with different rewiring probability

Average Error		$\rho = 0.1$	$\rho = 0.2$	$\rho = 0.3$	$\rho = 0.4$	$\rho = 0.5$	$\rho = 0.6$	$\rho = 0.7$	$\rho = 0.8$	$\rho = 0.9$	$\rho = 1$
$b_d, p_d > 0$	e_1	0.0598	0.0601	0.0612	0.0599	0.0654	0.0604	0.0617	0.065	0.0649	0.0654
	e_2	0.0333	0.034	0.0335	0.0329	0.0352	0.0331	0.0333	0.0345	0.0348	0.0344
$b_d, p_d = 0$	e_1	0.0472	0.0456	0.0475	0.0476	0.0475	0.0449	0.0452	0.0481	0.0445	0.0459
	e_2	0.0094	0.0091	0.0095	0.0095	0.0095	0.009	0.009	0.0096	0.0089	0.0092

We conclude that the rewiring probability has a negligible effect on the performance of the proposed control algorithm.

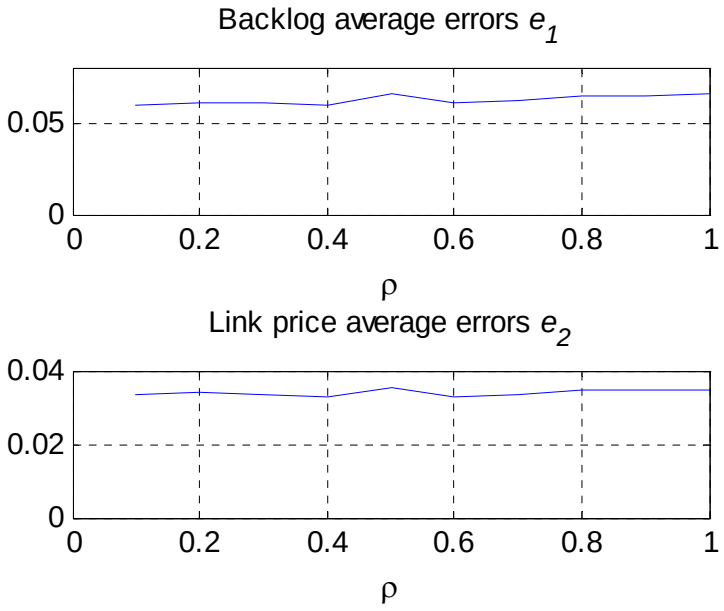

Figure 6.18. Average tracking errors as $b_l^d > 0$ and $p_l^d > 0$

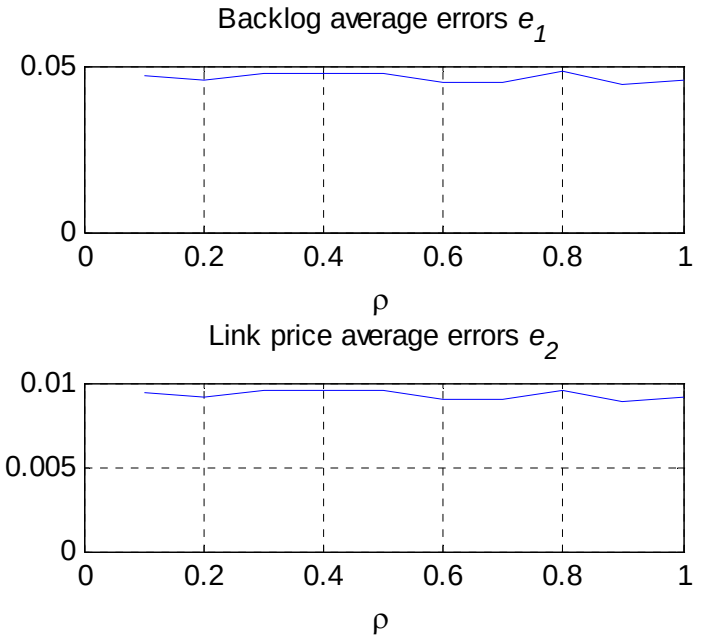

Figure 6.19. Average tracking errors as $b_l^d = 0$ and $p_l^d = 0$

CHAPTER 7
CONCLUSIONS AND FUTURE WORK

7.1 Conclusions

This work theoretically analyzed the adaptation, robustness and stability of flow control via source rate control as to regulate the link queue length and the link price. A simple adaptive control law that can cope with the effect of uncertainty and disturbance from unknown local traffic or from outside of the controlled network, while at the same time maintain robust asymptotic stability, was developed and simulated. This is one of the first attempts of applying robust control theory to network flows.

We tried to explore mathematical and analytical methods of network flow control to understand the behavior of stressed networks, as well as to demonstrate attributes such as robustness, adaptation, stability, and suppression of uncertainties and disturbances. The analysis and the simulations revealed the following:

1 The allowable equilibrium conditions were identified in Chapter 3 by analyzing the feature of the continuous-time nonlinear network model adopted in Chapter 2.

2 A novel model description in terms of the matrix notation was developed, and a comprehensive source rate control vector was designed in Chapter 4 based on a vector reminiscent of the sliding surface representation.

3 Global asymptotic stability under mild assumptions is guaranteed by theoretical proof.

4 Simulations in Chapter 4 and Chapter 5 conducted in Matlab illustrated that the proposed control laws ensured robust tracking of desired network dynamics with respect to both constant and realistic time-varying backbone source rates. The designed controller was also capable of mitigating the effect of uncertainties and disturbances from unknown local traffic sources and from outside of the controlled network. The proposed control laws exhibited promising tracking ability, adaptation and robustness.

5 More simulations were carried out in a more realistic small-world network in Chapter 6. Asymptotic stability and robust adaptation at equilibrium conditions of the proposed control schemes were observed in a large network. The rewiring probability seemed to have a negligible effect on tracking errors.

7.2 Future Directions

In the future, the robust adaptive control algorithms proposed in Chapter 4 will be extended to routing control. Routing protocols to achieve minimal communication time with minimum consumption of network resources will be studied. Delayed global stability with elastic link capacity will also be investigated.

Our effort will also be geared towards computational approaches that are amenable to real-time implementations, and able to respond robustly to congestion.

REFERENCES

[1] R. J. Ellison, D. A. Fisher, R. C. Linger, H. F. Lipson, T. Longstaff, N. R. Mead. "Survivable Network Systems: An Emerging Discipline." *Technical Report*, Software Engineering Institute, Carnegie Mellon University, Pittsburgh, PA, November 1997.

[2] S Kamolphiwong, A. E. Karbowiak, H. Mehrpour. "Flow control in ATM networks: a survey." *Computer Communications*, Volume 21, Issue 11, 951-968, August 1998.

[3] W. Fischer, E. Wallmeier, T. Worster, S. P. Davis, A. Hayter. "Data communications using ATM: architectures, protocols, and resource management." *IEEE Communications Magazine*, Volume 32, Issue 8, 24-33, August 1994.

[4] F. Kelly, A. Maulloo, and D. Tan. "Rate control in communication networks: Shadow prices, proportional fairness and stability." *The Journal of the Operational Research Society*, Volume 49, Issue 3, 237-252, March 1998.

[5] S. H. Low and D. E. Lapsley. "Optimization flow control—I: Basic algorithm and convergence." *IEEE/ACM Transactions on Networking*, Volume 7, Issue 6, 861-874, December 1999.

[6] S. H. Low. "A duality model of TCP and queue management algorithms." *IEEE/ACM Transactions on Networking*, Volume 11, Issue 4, 525-536, August 2003.

[7] W. Wang, M. Palaniswami, and S. H. Low. "Optimal flow control and routing in multi-path networks." *Performance Evaluation*, Volume 52, 119-132, 2003.

[8] J. Wang, L. Li, S. H. Low and John C. Doyle. "Cross-layer Optimization in TCP/IP Net-

works." *IEEE/ACM Transactions on Networking*, Volume13, Issue 3, 582-595, June 2005.

[9] F. Paganini. "On the stability of optimization-based flow control." *Proceedings of the American Control Conference*, Arlington, VA, Volume 6, 4689-4694, June 25-27, 2001.

[10] F. Paganini. "A global stability result in network flow control." *Systems & Control Letters*, Volume 46, Issue 3, 165-172, 5 July 2002.

[11] S. Athuraliya, V. Li, S.H. Low, Q. Yin. "REM: active queue management." *IEEE Network*, Volume 15, Issue 3, 48-53, May/June 2001.

[12] J. T. Wen and M. Arcak. "A unifying passivity framework for network flow control." *IEEE Transactions on Automatic Control*, Volume 49, Issue 2, 162-174, February 2004.

[13] F. Paganini. "Flow control via pricing: a feedback perspective." *Proceedings of the Allerton Conference*, Monticello, IL, October 2000.

[14] A. Iftar. "An Intelligent Control Approach to Decentralized Routing and Flow Control in High Ways." *Proceedings of the 12th IEEE Conference on International Symposium on Intelligent Control*, Istanbul, Turkey, 269-274, July 1997.

[15] A. Iftar. "A decentralized routing controller for congested highways." *Proceedings of the IEEE Conference on Decision and Control*, New Orleans, LA, 4089-4094, December 1995.

[16] P. E. Sarachik and U. Ozguner. "On decentralized dynamic Routing for congested traffic networks." *IEEE Transactions on Automatic Control*, Volume 27, Issue 6, 1233-1238, December 1982.

[17] R. Srikant. *The Mathematics of Internet Congestion Control*. Birkhäuser, Boston, MA, 2004.

[18] K. Collins and G. Muntean. “A vehicle route management solution enabled by wireless vehicular networks.” *IEEE INFOCOM*, 1-6, 2008.

[19] Dan A. Rosen, frank J. Mammano and Rinaldo Favout. "An Electronic Route-Guidance System for Highway Vehicles." *IEEE Transactions on Vehicular Technology,* Volume 19, Issue 1, 143-152, February 1970.

[20] Y. E. Hawas, H. S. Mahmassani. "Comparative Analysis of Robustness of Centralized and Distributed Network Route Control Systems in Incident Situations." *Transportation Research Record 1537,* 83-90, 1996.

[21] S. Glaser, B. Vanholme, S. Mammar, D. Gruyer, and L. Nouvelière. "Maneuver-Based Trajectory Planning for Highly Autonomous Vehicles on Real Road With Traffic and Driver Interaction." *IEEE Transactions on Intelligent Transportation Systems*, Volume 11, Issue 3, 589-606, September 2010.

[22] H. K. Khalil. *Nonlinear Systems*. Prentice Hall, Inc., Upper Saddle River, New Jersey, 2002.

[23] Y. D. Song. "Adaptive Motion Tracking Control of Robot Manipulators – Non-regressor Based Approach." *International Journal of Control*, Volume 63, Issue 1, 41-54, 1996.

[24] J. T. Spooner, K. M. Passino. "Stable Adaptive control Using Fuzzy Systems and Neural Networks." *IEEE Transactions on fuzzy systems*, Volume 4, Issue 3, 339-359, August 1996.

[25] Lloyd N. Trefethen and David Bau III. *Numerical linear algebra*. SIAM: Society for Industrial and Applied Mathematics, Philadelphia, PA, 1 June 1997.

[26] P. A. Ioannou and J. Sun. *Robust Adaptive control*. Prentice Hall, Inc., Upper Saddle River,

New Jersey, 1996 (Out of print in 2003). Electronic copy at http://www-rcf.usc.edu/~ioannou/Robust_Adaptive_Control.htm.

[27] Y. D. Song. "Adaptive parameter estimators for a class of non-linear systems." *International Journal of Adaptive Control and Signal Processing*, Volume 11, Issue 7, 641-648, November 1997.

[28] Augustin Soule, Antonio Nucci, Rene L. Cruz, Emilio Leonardi and NinaTaft. "Estimating Dynamic Traffic Matrices by Using Viable Routing Changes." *IEEE/ACM Transactions on Networking*, Volume 15, Issue 3, 485-498, June 2007.

[29] Duncan J. Watts, Steven H. Strogatz. "Collective dynamics of ‘small-world’ networks." *Nature*, Volume 393, Issue 6684, 440-442, 4 June 1998.